2003-12

Digital enhancement of night vision and thermal images

Teo, Chek Koon

Monterey, California. Naval Postgraduate School

NAVAL
POSTGRADUATE
SCHOOL

MONTEREY, CALIFORNIA

THESIS

DIGITAL ENHANCEMENT OF NIGHT VISION AND THERMAL IMAGES

by

Chek Koon Teo

December 2003

Co-Advisors: Monique P. Fargues
Alfred W. Cooper

Approved for public release; distribution is unlimited.

THIS PAGE INTENTIONALLY LEFT BLANK

REPORT DOCUMENTATION PAGE		Form Approved OMB No. 0704-0188

Public reporting burden for this collection of information is estimated to average 1 hour per response, including the time for reviewing instruction, searching existing data sources, gathering and maintaining the data needed, and completing and reviewing the collection of information. Send comments regarding this burden estimate or any other aspect of this collection of information, including suggestions for reducing this burden, to Washington headquarters Services, Directorate for Information Operations and Reports, 1215 Jefferson Davis Highway, Suite 1204, Arlington, VA 22202-4302, and to the Office of Management and Budget, Paperwork Reduction Project (0704-0188) Washington DC 20503.

1. AGENCY USE ONLY *(Leave blank)*	2. REPORT DATE December 2003	3. REPORT TYPE AND DATES COVERED Master's Thesis

4. TITLE AND SUBTITLE:
Digital Enhancement of Night Vision and Thermal Images

5. FUNDING NUMBERS

6. AUTHOR(S)
Mr Chek Koon Teo, Republic of Singapore

7. PERFORMING ORGANIZATION NAME(S) AND ADDRESS(ES)
Naval Postgraduate School
Monterey, CA 93943-5000

8. PERFORMING ORGANIZATION REPORT NUMBER

9. SPONSORING /MONITORING AGENCY NAME(S) AND ADDRESS(ES)
N/A

10. SPONSORING/MONITORING AGENCY REPORT NUMBER

11. SUPPLEMENTARY NOTES
The views expressed in this thesis are those of the author and do not reflect the official policy or position of the Department of Defense or the U.S. Government.

12a. DISTRIBUTION / AVAILABILITY STATEMENT
Approved for public release. Distribution is unlimited.

12b. DISTRIBUTION CODE
A

13. ABSTRACT (maximum 200 words)

Low image contrast limits the amount of information conveyed to the user. With the proliferation of digital imagery and computer interface between man-and-machine, it is now viable to consider digitally enhancing the image before presenting it to the user, thus increasing the information throughput. This thesis explores the effect of the Contrast Limited Adaptive Histogram Equalization (CLAHE) process on night vision and thermal images. With better contrast, target detection and discrimination can be improved. The contrast enhancement by CLAHE is visually significant and details are easier to detect with the higher image contrast. Analyzing the image frequency response reveals increases in the higher spatial frequencies. As higher frequencies correspond to image edges, the power increase is viewed as corresponding to edge enhancement and hence, an increase in visible image details. This edge enhancement is perceived as improvement in image quality. This is further substantiated by a subjective testing, where a majority of human subjects agreed that CLAHE-enhanced images are more informative than the original night vision images.

14. SUBJECT TERMS Image enhancement, night vision images, Contrast Limited Adaptive Histogram Equalization, CLAHE, contrast enhancement, image quality assessment.	15. NUMBER OF PAGES 93
	16. PRICE CODE

17. SECURITY CLASSIFICATION OF REPORT	18. SECURITY CLASSIFICATION OF THIS PAGE	19. SECURITY CLASSIFICATION OF ABSTRACT	20. LIMITATION OF ABSTRACT
Unclassified	Unclassified	Unclassified	UL

NSN 7540-01-280-5500

Standard Form 298 (Rev. 2-89)
Prescribed by ANSI Std. 239-18

THIS PAGE INTENTIONALLY LEFT BLANK

Approved for public release; distribution is unlimited.

DIGITAL ENHANCEMENT OF NIGHT VISION AND THERMAL IMAGES

Chek Koon Teo
Republic of Singapore
B.Eng, National University of Singapore, 1997

Submitted in partial fulfillment of the
requirements for the degree of

MASTER OF SCIENCE IN COMBAT SYSTEMS TECHNOLOGY

from the

NAVAL POSTGRADUATE SCHOOL
December 2003

Author: Chek Koon Teo

Approved by: Monique P. Fargues
Thesis Co-Advisor

Alfred W. Cooper
Thesis Co-Advisor

James H. Luscombe
Chairman, Department of Physics

THIS PAGE INTENTIONALLY LEFT BLANK

ABSTRACT

Low image contrast limits the amount of information conveyed to the user. With the proliferation of digital imagery and computer interface between man-and-machine, it is now viable to consider digitally enhancing the image before presenting it to the user, thus increasing the information throughput. This thesis explores the effect of the Contrast Limited Adaptive Histogram Equalization (CLAHE) process on night vision and thermal images. With better contrast, target detection and discrimination can be improved. The contrast enhancement by CLAHE is visually significant and details are easier to detect with the higher image contrast. Analyzing the image frequency response reveals increases in the higher spatial frequencies. As higher frequencies correspond to image edges, the power increase is viewed as corresponding to edge enhancement and hence, an increase in visible image details. This edge enhancement is perceived as improvement in image quality. This is further substantiated by a subjective testing, where a majority of human subjects agreed that CLAHE-enhanced images are more informative than the original night vision images.

THIS PAGE INTENTIONALLY LEFT BLANK

TABLE OF CONTENTS

LIST OF FIGURES

LIST OF TABLES

THIS PAGE INTENTIONALLY LEFT BLANK

ACKNOWLEDGMENTS

I am sincerely grateful to Professors Monique Fargues and Alfred Cooper for their wisdom, guidance and encouragement in completing this thesis.

I would also like to thank Professor Ronald Pieper for his guidance and advice during the initial stages of this thesis, before he left the Naval Postgraduate School.

Last but not least, I would like to acknowledge my lovely wife, Woonie. To her, I am indebted for her understanding and steadfast support in these difficult times. Without which, everything should not have been possible.

THIS PAGE INTENTIONALLY LEFT BLANK

I. INTRODUCTION

A. BACKGROUND

The element of surprise has long been touted as the main tactical advantage that would turn the tide of a battle. Throughout history, commanders have employed the darkness of night to gain surprise and to grasp the initiative from the hands of the enemy. Yet, while night operations have progressed from nocturnal maneuvers to the more recent firefights in Afghanistan and the “24-hour battlefield”, difficulties associated with night operations still plague all commanders, particularly the ability to see clearly and the ability to differentiate friend-or-foe. The fact remains that darkness is "a double-edged weapon", and like terrain, "it favors the one who best uses it and hinders the one who does not." [Sasso, 1982].

Human beings are visual and non-nocturnal creatures by nature. Not gifted with any special or hyper-sensitive sensory organs, they rely more on their ability to see than on any of the other four senses (smell, hear, touch and taste) to understand and manipulate their surroundings. The cone and rod photoreceptors in the human eye are responsible for generating these sought-for visionary senses. The rods are more numerous and more sensitive than cones in low levels of illumination (more than one thousand times). They basically contribute our limited night or scotopic vision. However, the rods are not sensitive to color like the cones, i.e. they only generate monochrome images. Hence, objects that appear brightly colored in daylight, when seen under moonlight appear as colorless forms, because only the rods are stimulated.

In the absence of artificial light sources, the main source of natural illumination at night comes from the moon and to a lesser degree, the stars (estimated at one-tenth of a quarter moon). The amount of luminance ranges from 0.1 lux (full moon) to 0.0001 lux (overcast night) [Sampson, 1996]. Depending on the reflectivity of the objects, the eventual irradiance on the human eye may not be high enough to even stimulate the rods.

However, if we explore beyond the visible light spectrum (400 -700 nm), the Infra-Red (IR) spectrum offers possibilities for exploitation as reflected in Figures 1 and 2. Both the night luminance and the foliage reflectivity are higher in the Near Infra-Red (NIR) band, i.e. there is more light energy in this wavelength band.

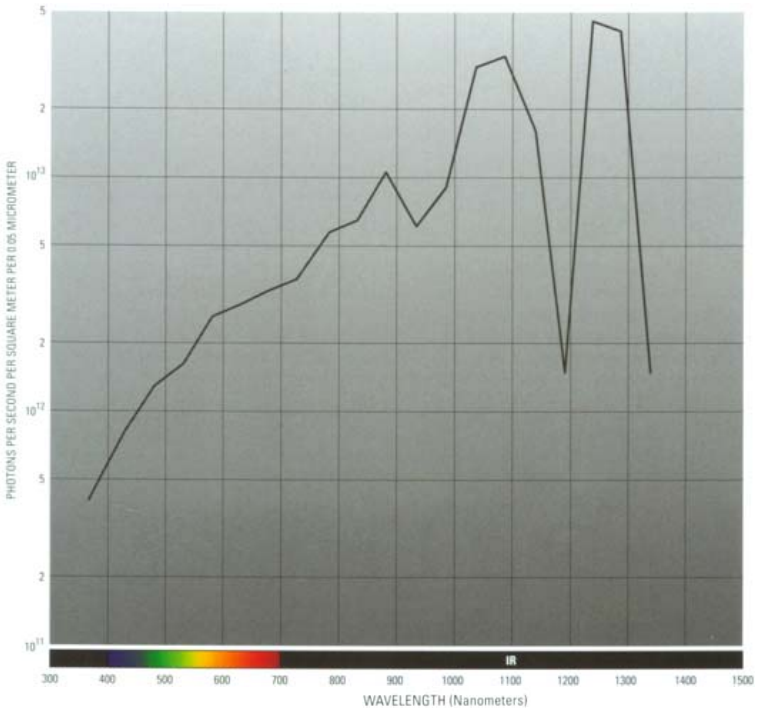

Figure 1: Natural night sky spectral irradiance, showing a higher irradiance in the NIR band [From Korry, 2003].

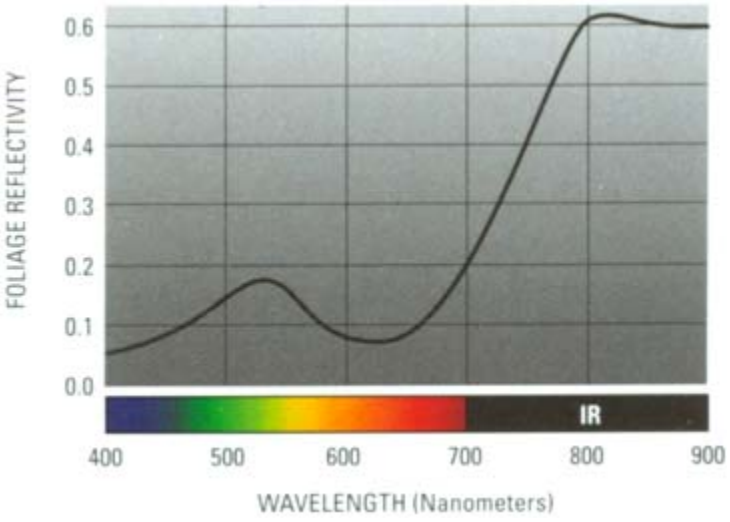

Figure 2: Foliage reflectivity: foliage is a better reflector in the IR band [From Korry, 2003].

Hence, if we were able to “sense” IR or near-IR radiation (which the human photoreceptors are unable to do naturally), our night vision capability would be immediately improved, given the higher luminance available.

B. NIGHT VISION

There are two basic methods to improve night vision. The first is to increase the amount of visible light reaching the eye, as with artificial lighting such as a flashlight or by converting the “otherwise-invisible” radiation to visible radiation. The second is through light amplification, i.e. by increasing the normally imperceptible radiation energy to a level detectable by the human eyes. These methods to achieve night imagery are employed by the Image Intensifier (II) and the Thermal Imager (TI).

1. Image Intensifier

As the name implies, Image Intensifiers (II) are designed to boost very low intensity optical images to the point where they become perceivable to the human eye. They also act as wavelength “down-converters”, that is they convert near-IR radiation into visible radiation. II devices are commonly known as Night Vision Device (NVD) or Night Vision Goggles (NVG), depending on the mode of usage.

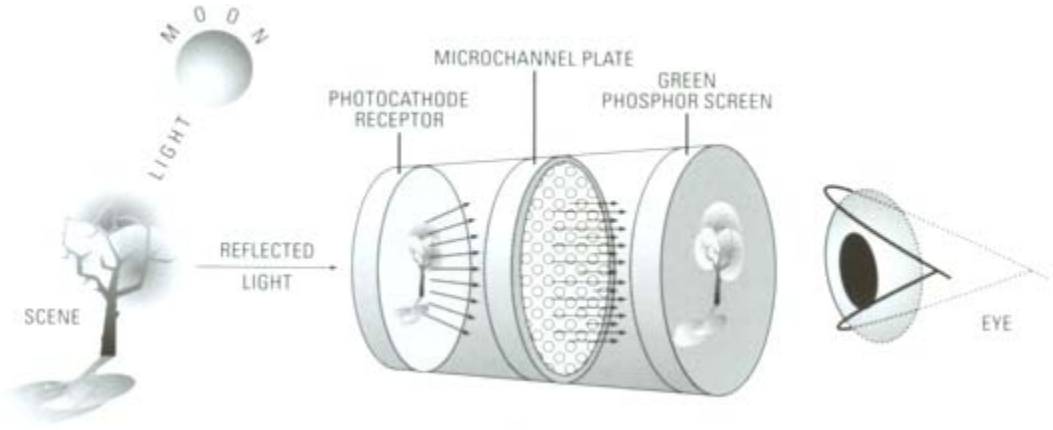

Figure 3: A Night Vision Device with the light amplifying microchannel plate [From Korry, 2003].

A typical II system consists of three main components: the photocathode, the micro-channel plate (MCP) and the phosphor screen, as shown in Figure 3. Reflected light from the scene or object enters the device and is focused onto the photocathode by an optical lens system. Photons striking the photocathode surface release photo-electrons. The flux of photo-electrons generated is proportional to the flux of incident light photons and the responsivity of the photocathode. In the first-generation of NVDs, the energy of the photo-electron is increased by acceleration with an externally applied electric field. Second-generation devices make use of the MCP to achieve energy gain through electron multiplication. The actual number of photo-electrons is multiplied by accelerating the electrons through the MCP where an “avalanche” of secondary electrons is produced as a result of collisions between the electrons and the MCP wall. On emerging from the MCP, the electrons strike a phosphor screen which emits visible light, hence creating a visible image to the human eye. The most commonly-used phosphor is KA(P20) as it emits a greenish light at 560 nm, matching the peak sensitivity of the human eye. Furthermore, the P20 has fast decay time and high conversion efficiency, which is ideal for night vision purpose [Ji, 2002].

The newer generation (Gen III) of NVDs uses a Gallium Arsenide (GaAs) photocathode which is sensitive to light beyond 800 nm and where the night sky illuminance levels are also higher (Figure 1). The MCP used in the third-generation NVDs is also much smaller in pitch, thus giving better spatial resolution. As a result, Gen III NVDs can deliver a three-fold improvement in visual acuity and detection distances over the earlier generations. The light amplification achievable could be 30,000 times or more [LCEO, 2003].

2. Thermal Imager

All material objects with temperatures above absolute zero Kelvins radiate infrared energy. A Thermal Imager (TI) detects this radiation (including reflected infrared energy) and converts this energy into a visible presentation. The commonest class of TI systems is the Forward-Looking Infrared system (FLIR). A system operating in the 8- to 14-μm region is usually referred to as an LWIR (long-wavelength infrared) FLIR, and one operating in the 3- to 5-μm as a MWIR (medium-wavelength infrared) FLIR. These are the two transmission windows where atmospheric attenuation of infrared radiation is minimal.

Most IR detectors operate using quantum mechanical interaction between incident photons and detector material. Photoconductive detectors absorb photons to elevate electrons from the valence band to the conduction band of the material, changing the conductivity of the detector. Photovoltaic detectors absorb photons to create electron hole pairs across a p-n junction which produces a small current. Such devices can be manufactured as part of an array that includes a capacitor that stores a charge proportional to the incident radiation. The charged array can then be read or scanned to produce the corresponding image.

As the TI senses temperature difference or contrast (sensitivity is frequently defined in terms of Minimum Resolvable Temperature Difference), detectors with small band-gap energies must be cooled to minimize thermally generated carriers and inherent detector noise.

The bolometer is a thermal detector that absorbs thermal energy over all wavelengths and changes its resistance accordingly. The change in resistance will produce a change in electric current which can be monitored. The radiation to the bolometer is usually modulated to improve sensitivity and uniformity [Holst, 2003].

C. CONTRAST SENSITIVITY

The difference in radiation intensity levels (both emitted and reflected) from a scene creates the information contained within an image. An object of interest can be identified by its contrast against its immediate surroundings, which defines the object's boundaries and edges. Contrast is defined as the difference in luminance or radiation intensity levels between regions or pixels.

The larger the contrast, the easier an object can be detected from the scene. This can be illustrated by Figure 4, a Contrast Sensitivity Function (CSF) test image produced by Campbell and Robson in 1968.

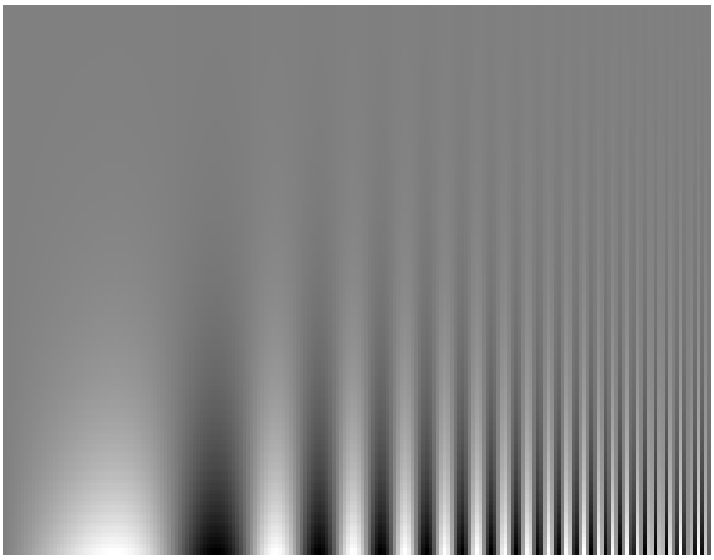

Figure 4: Contrast Sensitivity Function test chart by Campbell-Robson [From McCourt, 2003].

In Figure 4 above, spatial frequency increases from left to right (the bars become thinner and thinner) and contrast decreases from bottom to top (difference in gray level between the bars and background decreases). From a fixed viewing distance, note the contrast values where the bars are just barely visible over the range of spatial frequencies. Trace these out to form an inverted U-shaped curve and this will represent your contrast sensitivity function. The

region below the U-shaped curve is the visible stimuli region, where objects of such combination of spatial frequency and contrast will be detectable by the eye. The CSF of a typical adult human is shown in Figure 5 for reference. The influence of contrast on visible stimulus and object detection is evident.

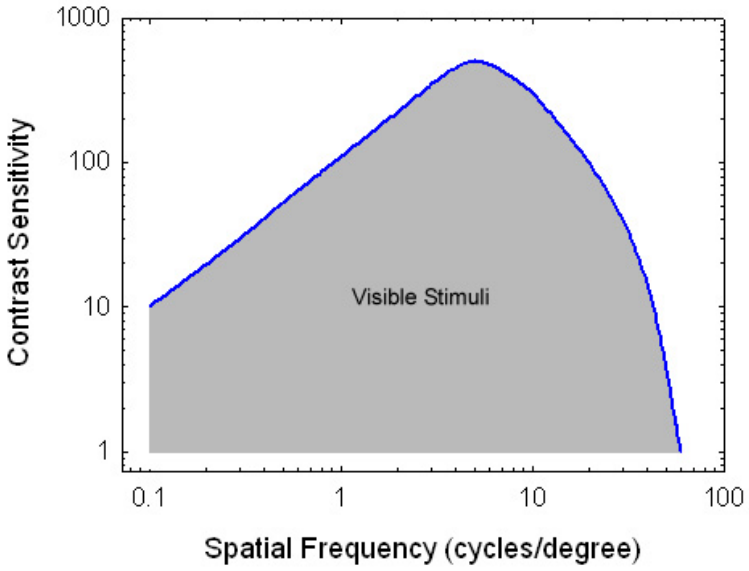

Figure 5: CSF of adult human. Contrast sensitivity is defined as the inverse of contrast threshold, which is the minimum contrast level to see the grating in the test image [From McCourt, 2001].

1. II Imagery

Figure 6 is a typical II image obtained by a NVD or NVG. As discussed in the previous section, the low luminance, coupled with low reflectivity from the ground and foliage, generates a low-contrast image with limited dynamic contrast range. Detector noise and clutter from the background degrades the image further. Figure 6 also shows a lack of details and contrast in the ground before the treeline, which are essential for situational awareness and navigation. However, the upper portion of the image has better contrast due to illumination by the night sky (from moon and stars). In this more illuminated region, the foliage can be differentiated, as the objects would be within the CSF for detection.

Figure 6: A NVD image [From Naval Research Laboratory (NRL)].

Figure 7: A TI image [From NRL].

2. TI Imagery

Figure 7 is a FLIR or TI image of the same scene as Figure 6. The temperature difference between the regions (due to different cooling rates of the earth or soil) generates sufficient contrast to see the layout of the ground before the treeline. The warm air and the low emissivity of the trees also creates the sharp contrast cues of the treeline against the sky (the treeline appears darker). However, for areas of homogeneity in temperature or emissivity (such as the foliage of individual trees), there is a lack of contrast or surface information, as evident by the “hollow appearance” of the foliage. Note that the IIs do not have this problem, as they detect the reflected radiation from the surface of the objects. Hence, the information contained in the II and TI images is complementary since the sensors operate in different bands of the electromagnetic spectrum. This leads to the impetus for image or sensor fusion to improve image quality and content [Scrofani, 1997].

3. Comparison of TI and II Imagery

In a military context, the object of interest tends to be either man-made or alive. Such objects will have a temperature above zero Kelvin, due to body heat or some other energy generating process. Without solar heating, the air and the earth cool down during the night. Hence, all these objects of interest will contrast easily against the background and stand out in a TI, unless there is deliberate action to reduce the temperature contrast (such as camouflaging or shielding). In comparison, II depends greatly on ambient light (artificial or natural) for visibility, as it amplifies reflected incoming light. Therefore, in a totally dark room, the II will not be able to generate any image at all, whilst the TI is still able to “see”, provided that there are temperature gradients present. The TI also has better ability to see through smoke, rain and snow, as the longer wavelength IR radiation is able to propagate in the presence of such atmospheric particles with minimal attenuation, unlike shorter visible and near-IR radiation which would be scattered. As a result, the detection range for TI tends to be greater than II.

As II intensifies and amplifies incoming light, there is a possibility of "overloading" the II detector by a bright or high luminance source, which could temporarily "black-out" the sensor, similar to human vision when stepping out from a dark room into bright sunlight. The II is designed to "see" at night where the luminance level is low (0.1 lux or lower). Hence, a source with an intensity level a couple of orders of magnitude higher is sufficient to overload the II baseline sensitivity (a handheld flashlight is capable of producing 100 lux or more). Although the MCP amplifier generally has a non-linear response which reduces gain response at high irradiance, it is still insufficient to isolate bright sources and avoid such saturation. Figure 8 is a representation of this "over-exposure" pitfall of the II by a light source.

Figure 8: An II image degraded by over-exposure [From NRL].

Figure 9: A TI image of the same scene as Figure 8, displaying better contrast and details level than the II image [From NRL].

Given the tactical advantages of TI and the shortcomings of II, there is therefore a general preference for TI as the night vision sensor of choice for detection. However, II still has a slight advantage in identification, because of its ability to sense surface differences from their reflectivity. The relatively lower cost and compactness of II systems make them attractive for field deployment, as unlike the TI systems, they do not require a cooling system for better sensitivity.

In general, due to limited reflectivity characteristics from the scene, the quality of II images is hampered by lower contrast. It is difficult to discriminate objects from the background and clutter. From the previous section, increasing the contrast increases the visible stimulus and the probability of detection, as demonstrated by the Contrast Sensitivity Function (CSF) in Figure 5. Therefore, the usability of II system for detection will be enhanced if the contrast of the II images can be improved or the dynamic range expanded, without altering the spatial content of the original image.

D. OBJECTIVE

Image enhancement techniques to improve visual quality have been popularized with the proliferation of digital imagery and computers. Techniques range from noise filtering, edge enhancement, color balance and contrast enhancement, in both frequency and spatial domains. Even in word processor software such as Microsoft Word, there are features or tool options to manipulate contrast and brightness levels of images.

Computer-aided operation is also becoming a necessity, even in the military. Advanced systems and arms modernization programs often involve the integration of a computer or a computer processing interface to reduce the combat loading on the soldier or improve system reaction time. One prime example is the Land Warrior program [FAS website, 2003], where communications, sensors, and materials are integrated into a complete soldier system. At the heart of this soldier system, is a computer module or subsystem which integrates all the information and sensors together before presenting to the soldier via a helmet mounted display. The electro-optical sensors include thermal weapon sight, image intensifier, video camera (visible) and laser range-finder. Electro-optical sensors are also generally transitioning from direct view to remote display, which provides a possibility for enhancement.

Taking the two developments in stride, it is therefore feasible to digitally enhance the night vision images with a computer algorithm before presenting it to the user, particularly a military one. Images acquired from the night vision device can be easily digitized by coupling the sensor output screen to a scanning array or an Analog-to-Digital converter. Next, the digital image can undergo a contrast enhancement algorithm, such as the Contrast-Limited Adaptive Histogram Equalization (CLAHE) to improve its visible scene content, while maintaining the spatial relation of the original image, before displaying the final improved image to the human user.

II systems and images would benefit most from such a contrast enhancement because of their inherent low contrast limitation. The II system

would be given a new life and a new “light” per se, when the quality of the II images can be improved significantly by the proposed algorithm. Furthermore, no major modification is required on the II system since the enhancement is done by a software algorithm.

This thesis explores the effect of such an image enhancement algorithm on the night vision image. Chapter II briefly reviews the fundamentals of digital image processing and the CLAHE process, while Chapter III analyses the enhancement results obtained with the CLAHE process. Finally, Chapter IV presents the conclusions and recommendations for further research.

THIS PAGE INTENTIONALLY LEFT BLANK

II. DIGITAL IMAGE PROCESSING

A. DIGITAL IMAGE

A digital image is essentially a two-dimensional array of light-intensity levels, which can be denoted by *f(x,y)*, where the value or amplitude of *f* at spatial coordinates *(x,y)* gives the intensity of the image at the point. The intensity is a measure of the relative "brightness" of each point. The brightness level is represented by a series of discrete intensity shades from darkest to brightest, for a monochrome (single color) digital image. These discrete intensity shades are usually referred to as the "gray levels", with black representing the darkest level and white, the brightest level. These levels will be encoded in terms of binary bits in the digital domain, and the most commonly used encoding scheme is the 8-bit display with 256 levels of brightness or intensity, starting from level 0 (black) to 255 (white). The digital image can therefore be conveniently represented and manipulated as an N (number of rows) x M (number of columns) matrix, with each element containing a value between 0 and 255 (for an 8-bit monochrome image), i.e.

$$f(x,y)=\begin{bmatrix} f(0,0) & f(1,0) & . & . & f(0,M-1) \\ f(1,0) & f(1,1) & . & . & f(1,M-1) \\ . & . & . & . & . \\ . & . & . & . & . \\ f(N-1,0) & f(N-1,1) & . & . & f(N-1,M-1) \end{bmatrix}, \text{ where } 0 \le f(x,y) \le 255.$$

Different colors are created by mixing different proportions of the 3 primary colors: red, green and blue, i.e. RGB for short. Hence, a color image is represented by an N x M x 3 three-dimensional matrix, with each layer representing the gray-level distribution of one primary color in the image.

Each point in the image denoted by the *(x,y)* coordinates is referred to as a pixel. The pixel is the smallest cell of information in the image. It contains a

value of the intensity level corresponding to the detected irradiance. Therefore, the pixel size defines the resolution and acuity of the image seen. Each individual detector in the sensor array and each dot on the LCD (liquid crystal display) screen contributes to generate one pixel of the image. There is actually a physical separation distance between pixels due to finite manufacturing tolerance. However, these separations are not detectable, as the human eye is unable to resolve such small details at normal viewing distance (refer to Rayleigh's criterion for resolution of diffraction-limited images [Pedrotti, 1993]). For simplicity, digital images are represented by an array of square pixels.

The relation between pixels constitutes the information contained in an image. A pixel at coordinates *(x,y)* has eight immediate neighbors which are a unit distance away:

(x-1, y-1)	*(x-1, y)*	*(x-1, y+1)*
(x, y-1)	*(x,y)*	*(x, y+1)*
(x+1, y-1)	*(x+1, y),*	*(x+1, y+1)*

Figure 10: Neighbors of a Pixel. Note the direction of the *x* and *y* coordinates used.

Pixels can be connected to form boundaries of objects or components of regions in an image when the gray levels of adjacent pixels satisfy a specified criterion of similarity (equal or within a small difference). The difference in the gray levels of two adjacent pixels gives the contrast needed to differentiate between regions or objects. This difference has to be of a certain magnitude in order for the human eye to identify it as a boundary.

B. IMAGE PROCESSING METHODS

There are two main methods to process an image as defined by the domain in which the image is processed, namely the spatial domain or the frequency domain. The spatial domain refers to the image plane itself, and approaches in this category are based on direct manipulation of pixels in an image. Frequency domain processing techniques are based on modifying the spatial frequency spectrum of the image as obtained by the Fourier transform. Enhancement techniques based on various combinations of methods from these two categories are not unusual and the same enhancement technique can also be implemented in both domains, yielding identical results [Gonzalez and Woods, 1993].

1. Spatial Domain Methods

The spatial domain refers to the aggregate of pixels composing an image, and spatial domain methods are procedures that operate directly on these pixels. Image processing functions in the spatial domain may be expressed as:

$$g(x,y) = T[\, f(x,y)\,], \tag{1}$$

where $f(x,y)$ is the input image data, $g(x,y)$ is the processed image data, and T is an operator on f, defined over some neighborhood of (x,y). In addition, T can also operate on a set of input images, for example performing the pixel-by-pixel sum and averaging a number of images for noise reduction.

The principal approach to defining a neighborhood about (x,y) is to use a square or rectangular mask centered at (x,y). The center of this mask or window is moved from pixel to pixel, and the operator applied at each location (x,y) to yield the corresponding g for that location. The resultant $g(x,y)$ is stored separately, instead of changing pixel values in place, to avoid a “snow-balling” effect of the altered gray levels.

2. Frequency Domain Methods

The foundation of frequency domain techniques is the convolution theorem. The processed image, $g(x,y)$, is formed by the convolution of an image $f(x,y)$ and a linear, position-invariant operation $h(x,y)$, that is

$$g(x,y) = h(x,y) * f(x,y). \quad (2)$$

By the convolution theorem, the following frequency domain relation holds:

$$G(u,v) = H(u,v)\, F(u,v), \quad (3)$$

where G, H, and F are the Fourier transforms of g, h and f respectively. $H(u,v)$ is called the transfer function of the process. In a typical image enhancement application, $f(x,y)$ is given and the goal, after computing $F(u,v)$, is to select a $H(u,v)$ so that the desired image $g(x,y)$ exhibits some highlighted feature of $f(x,y)$, i.e.

$$g(x,y) = F^{-1} [\, H(u,v)\, F(u,v)\,]. \quad (4)$$

For instance, edges in $f(x,y)$ can be accentuated by using a function $H(u,v)$ that emphasizes the high-frequency components of $F(u,v)$.

3. Global and Local Methods

Image processing methods that involve using a single transformation function for the whole image are classified as global methods or algorithms. The lowpass/highpass filters and histogram transformation are examples of global enhancement methods. The main advantage of global methods is that they are computationally inexpensive and simple to implement. However, global methods may attenuate or miss local information while working on the overall characteristic of the image.

The transformation function of a local processing method is dependent on the location and the neighborhood of the pixel looked at, i.e.

$$g(x,y) = T[x,y, f(x,y)]. \quad (5)$$

These methods are therefore “adaptive” to the local information within the image. Adaptive histogram equalization is an example of such a local processing method and is effective in enhancing details in local areas of the image. However, pixels of the same gray level in the original image may be mapped to different gray levels in the output image, due to the various “localized” mapping or transformation functions, which could artificially alter the appearance of the original image. Abrupt changes or boundaries may also result in the image, because each transformation is done locally and independently.

C. FILTERS

Filtering refers to the selective processing of an image to remove unwanted aspects of the image or to transform only certain portions of the image. Lowpass filters attenuate or eliminate high-frequency components in the Fourier domain, while allowing low frequencies to pass through untouched. As the high frequency components characterize edges and other sharp details in an image, the net effect of lowpass filtering is image blurring [Gonzalez and Woods, 1993]. Hence, lowpass filters are also known as smoothing filters and are commonly used for noise reduction.

Similarly, highpass filters attenuate low-frequency components. Because these components are responsible for the slowly varying characteristics of an image, such as overall contrast and average intensity, the net result of highpass filtering is a reduction of these features and a corresponding apparent sharpening of edges and other sharp details. Highpass filters are therefore known also as sharpening filters.

1. Lowpass Filtering

As indicated earlier, edges and other sharp transitions (such as noise) in the gray levels of an image contribute significantly to the high-frequency content of its Fourier transform. Hence, blurring or smoothing is achieved in the frequency domain by attenuating a specified range of high-frequency components in the transform of a given image.

A 2-D ideal lowpass filter is one whose transfer function in equation (4) satisfies the relation:

$$H(u,v) = \begin{cases} 1 & \text{if } D(u,v) \le D_0 \\ 0 & \text{if } D(u,v) > D_0 \end{cases}, \tag{6}$$

where D_0 is a specified non-negative quantity and $D(u,v)$ is the distance from point (u,v) to the origin of the frequency plane, i.e.

$$D(u,v) = (u^2 + v^2)^{1/2}. \tag{7}$$

The point of transition between $H(u,v) = 1$ and $H(u,v) = 0$, D_0, is called the cutoff frequency. One way to establish this cutoff frequency is to define the percent of signal power to be contained within or passed by the filter. D_0 is then equivalent to the radius of a circle with origin at the center of a 2-dimensional frequency plot. For an ideal filter, this transition is an impulse step, i.e. frequencies equal to or less than D_0 are passed with no attenuation, while frequencies higher than D_0 are completely attenuated. However, this sharp cutoff frequency cannot be realized with electronic components.

The Butterworth lowpass filter was formulated to address this practical limitation, as it does not have a sharp discontinuity between passed and filtered frequencies. The Butterworth transfer function (of order n) is defined as follows [Gonzalez and Woods, 1993]:

$$H(u,v) = \frac{1}{1 + [D(u,v)/D_0]^{2n}}. \tag{8}$$

Lowpass smoothing fliters can also be implemented in the spatial domain. Figure 11 shows a general 3x3 linear mask with arbitrary coefficients (weights) z. Denoting the gray levels of pixels under the mask at any location by $z_1, z_2 \ldots z_9$, the response of the mask is:

$$R = w_1 z_1 + w_2 z_2 + \ldots + w_9 z_9. \tag{9}$$

W_1	W_2	W_3
W_4	W_5	W_6
W_7	W_8	W_9

Figure 11: A 3x3 spatial mask with arbitrary coefficients [From Gonzalez and Woods, 1993].

All the coefficients of the mask are set to a value of 1 for simple smoothing processing. The response from the mask would be the sum of gray levels for the nine pixels under the mask, as per equation (8). This response *R* is then scaled down by dividing by the total number of pixels (nine in this case) to keep within the original gray levels range. Therefore, the response or result would simply be the average of all the pixels in the area of the mask. Larger masks (e.g. 5x5 and 7x7) follow the same concept and will blur the image further with larger neighborhood averaging. For the border pixels of the image, there will be a shortage of neighborhood pixels for the mask. One option is to pad the shortage with pixels of the same values as the center pixel or a reference pixel. Another option is to process one layer less of pixels, i.e. no filtering on the border pixels.

Lowpass filters are generally used for blurring and for noise reduction in preprocessing steps, such as the removal of small details from an image prior to object extraction, and bridging of small gaps in lines or curves. Figure 12 illustrates the effect of a lowpass filter.

Figure 12: Lowpass filtering with a 3x3 spatial filter or 98% percent power D_0 locus. The top image is the original image and the bottom the processed image, where the image details have been blurred.

2. Highpass Filtering

Image sharpening can be achieved in the frequency domain by a highpass filtering process as edges and other abrupt changes in gray levels are associated with high-frequency components. Such filtering attenuates the low-frequency components without disturbing high-frequency information in the Fourier transform. Highpass fliters are therefore known also as sharpening fliters.

The highpass filtering process can be implemented in both the frequency and spatial domains. For highpass filtering in the frequency domain, the transfer function is essentially the inverse of that obtained for lowpass filtering,

$$H(u,v) = \begin{cases} 0 & \text{if } D(u,v) \le D_0 \\ 1 & \text{if } D(u,v) > D_0 \end{cases}. \tag{10}$$

The transfer function of the Butterworth highpass filter of order n and with cutoff frequency locus at distance D_0 from the origin is defined by the relation

$$H(u,v) = \frac{1}{1 + [D_0 / D(u,v)]^{2n}}. \tag{11}$$

The principal objective of sharpening is to highlight fine detail in an image or to enhance detail that has been blurred, either in error or as a natural effect of a particular method of image acquisition. Uses of image sharpening vary and include applications ranging from electronic printing to medical imaging to industrial inspection and autonomous object detection.

A basic 3x3 highpass spatial mask is shown in Figure 13. The center coefficient is positive while the rest of the mask contains negative coefficients. The sum of the coefficients is then equal to zero. Thus, the output of the mask is zero or very small when the mask is over an area of constant or slowly varying gray level. As with highpass frequency filtering, the zero-frequency term is attenuated or eliminated. This will reduce the average gray-level value in the image to zero, which in turn reduces the global contrast of the image. The expected result from such a highpass mask is therefore characterized by highlighted edges over a dark background. Reducing the average value of an

image to zero also implies that the image may have negative gray levels due to the negative coefficients in the mask. Next, the results have to be adjusted or clipped and scaled down (by dividing by the number of pixels in the mask) to keep the output within the original (non-negative) gray level range.

-1	-1	-1
-1	8	-1
-1	-1	-1

Figure 13: A basic highpass spatial filter [From Gonzalez and Woods, 1993].

A highpass filtered image can be computed as the difference between the original image and a lowpass filtered version of the same image, as the highpass filter is the complement of the lowpass, i.e.,

$$Highpass = Original - Lowpass. \tag{12}$$

Multiplying the original image by an amplification factor, denoted by A, yields the definition of a high-boost or high-frequency-emphasis filter, i.e.,

$$\begin{aligned} Highboost &= (A)(Original) - Lowpass, \\ &= (A-1)(Original) + Original - Lowpass, \\ &= (A-1)(Original) + Highpass. \end{aligned} \tag{13}$$

When $A > 1$, part of the original is added back to the highpass result, which restores partially the low-frequency components lost in the highpass filtering operation. The result is that the high-boost image looks more like the original image, with a relative degree of edge enhancement that depends on the value of A. Therefore, the center weight of the high-boost filter can be represented by

$$W_5 = 9A-1 \quad with\ A \geq 1. \tag{14}$$

When $A = 1$, the basic highpass filter is obtained as in Figure 13 [Gonzalez and Woods, 1993].

Figure 14: High-boost filtering with A = 1.8. The bottom image is the processed image. The brightness of the image is lowered and the features of the ships sharpened.

D. HISTOGRAM

An image histogram is a plot of the distribution of intensities or gray levels in an image. The histogram of a digital image with gray levels in the range [0, *L*-1] can be represented by the discrete function

$$p(r_k) = \frac{n_k}{n}, \tag{15}$$

where r_k is the k^{th} gray level, n_k is the number of pixels in the image with that gray level, n is the total number of pixels in the mage, and k = 0, 1, 2, … L-1.

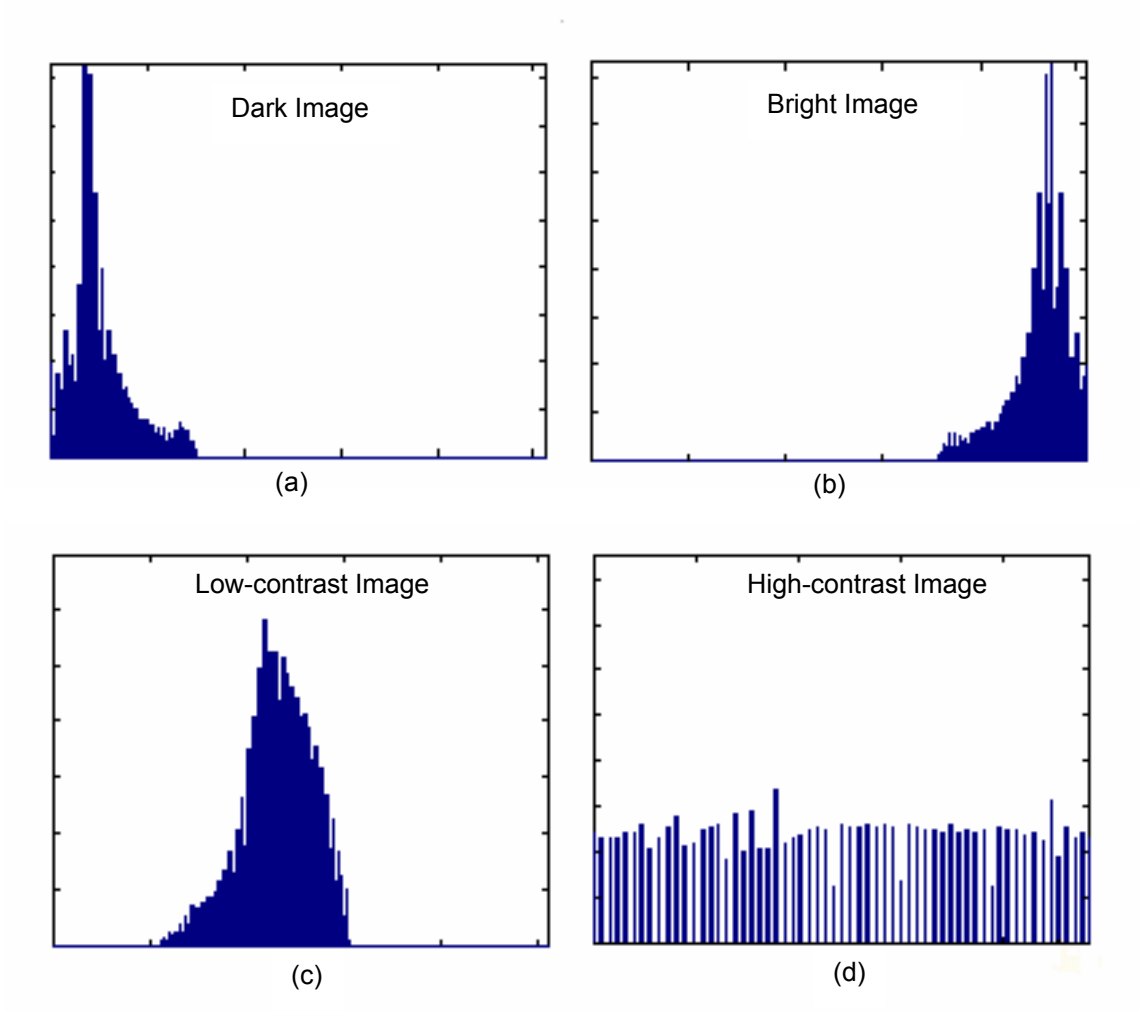

Figure 15: Histograms of four basic image types [After Gonzalez and Woods, 1993].

The image histogram gives an estimate of the probability of occurrence of a gray level r_k. A plot of this function for all values of k also provides a global description of the appearance of an image. For example, Figure 15 shows the histograms of four basic types of images. The histogram in Figure 15(a) shows that the gray levels are concentrated toward the dark end of the gray scale range. Thus, this histogram corresponds to an image with overall dark characteristics. Figure 15(b) is the opposite, with a bright image. The histogram shown in Figure 15(c) has a narrow shape, which indicates little dynamic range and thus corresponds to an image having low contrast, while Figure 15(d) shows a histogram with significant spread, corresponding to an image with high contrast.

Although the histogram does not provide any specific information about the image content, the shape and distribution of the histogram provide a venue for contrast enhancement. However, the histogram is a global representation of the intensity characteristics within an image and therefore, histogram transformation affects the whole image, i.e. globally. This differs from the localized methods such as the spatial mask and filters, which depend only on the pixel looked at and its neighbors.

E. HISTOGRAM EQUALIZATION

The histogram of an image represents the relative frequency of occurrence of gray levels within an image. It also represents the probability of such an occurrence. With a narrow distribution of gray levels (refer to Figure 15(c)), the contrast in the image will be low and the dynamic range limited. Hence, a good gray level assignment scheme would be to expand the intensity range to fill the whole dynamic range available. The probability of occurrence of all gray levels should be equal or uniform. In histogram equalization, the goal is to obtain a uniform histogram distribution for the output image, so that an optimal overall contrast is perceived.

An outline of the histogram equalization process is as follows [Gonzalez and Woods, 1993]:

Let the variable *r* represent the gray levels in the image to be enhanced or equalized. The pixel values can be normalized to form continuous quantities in the interval [0, 1], with $r = 0$ representing black and $r = 1$ representing white.

For any *r* in the interval [0, 1], the transformation is of the form:

$$s = T(r), \tag{16}$$

which produces a gray level *s* for every level of *r* in the original image. It is assumed that the transformation function given in equation (15) satisfies the conditions: (a) $T(r)$ is single-valued and monotonically increasing in the interval $0 \leq r \leq 1$; and (b) $0 \leq T(r) \leq 1$ for $0 \leq r \leq 1$. Condition (a) preserves the order from black to white in the gray scale, whereas condition (b) guarantees a mapping that is consistent with the allowed range of gray levels.

The inverse transformation from *s* back to *r* is then denoted

$$r = T^{-1}(s), \quad 0 \leq s \leq 1, \tag{17}$$

where the assumption is that $T^{-1}(s)$ also satisfies conditions (a) and (b) with respect to the variable *s*.

The gray levels in an image may be viewed as random quantities in the interval [0, 1]. If they are continuous variables, both the original and transformed gray levels can be characterized by their probability density function $p_r(r)$ and $p_s(s)$ respectively, where the subscripts on *p* are used to indicate that p_r and p_s are different functions.

The probability density function of the transformed gray levels can therefore be expressed by:

$$p_s(s) = \left[p_r(r) \frac{dr}{ds} \right]_{r=T^{-1}(s)}. \tag{18}$$

Consider the transformation function

$$s = T(r) = \int_0^r p_r(w)dw, \qquad 0 \le r \le 1, \tag{19}$$

where w is a dummy variable of integration. Equation (19) is actually the cumulative distribution function (CDF) of r. Conditions (a) and (b) presented earlier are satisfied by this transformation function, because the CDF increases monotonically from 0 to 1 as a function of r.

From equation (19), the derivative of s with respect to r is

$$\frac{ds}{dr} = p_r(r). \tag{20}$$

Substituting equation (20) into equation (18) yields

$$p_s(s) = \left[p_r(r) \frac{1}{p_r(r)} \right]_{r=T^{-1}(s)} = 1, \quad 0 \le s \le 1, \tag{21}$$

which gives a uniform density in the interval of the transformed variable s. This result is independent of the inverse transformation function. Thus, using the cumulative distribution function of r as the transformation function produces an image with uniform density gray levels and with better contrast distribution.

For discrete formulation, the probabilities are replaced by:

$$p(r_k) = \frac{n_k}{n} \quad 0 \le r_k \le 1 \text{ and } k = 0, 1 \ldots L\text{-}1, \tag{22}$$

and equation (19) will be given by the relation

$$s_k = T(r_k) = \sum_{j=0}^{k} \frac{n_j}{n} = \sum_{j=0}^{k} p_r(r_j). \tag{23}$$

A MATLAB implementation for the histogram equalization is available in Appendix A.

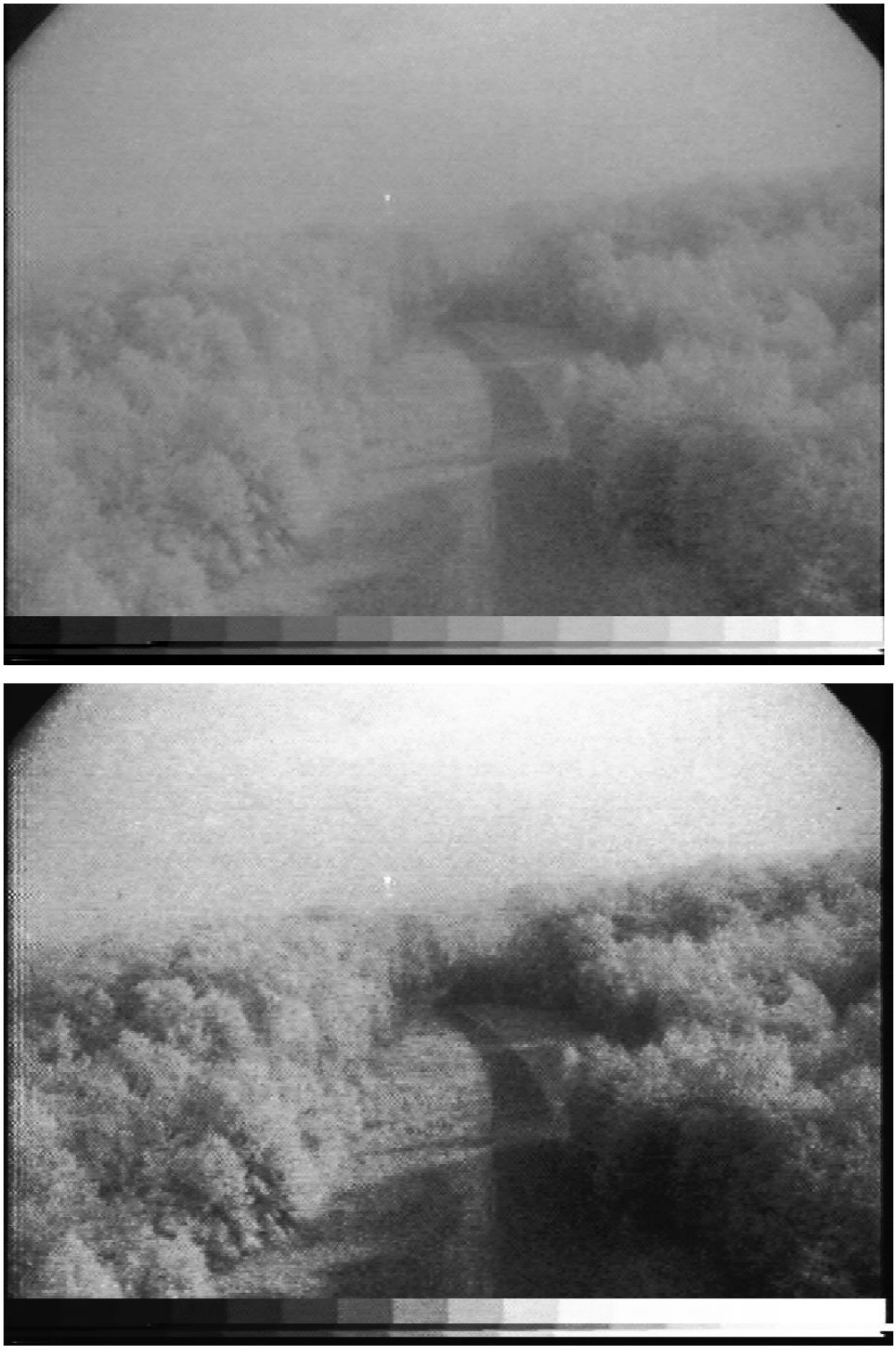

Figure 16: Result of histogram equalization. The bottom image is the processed output.

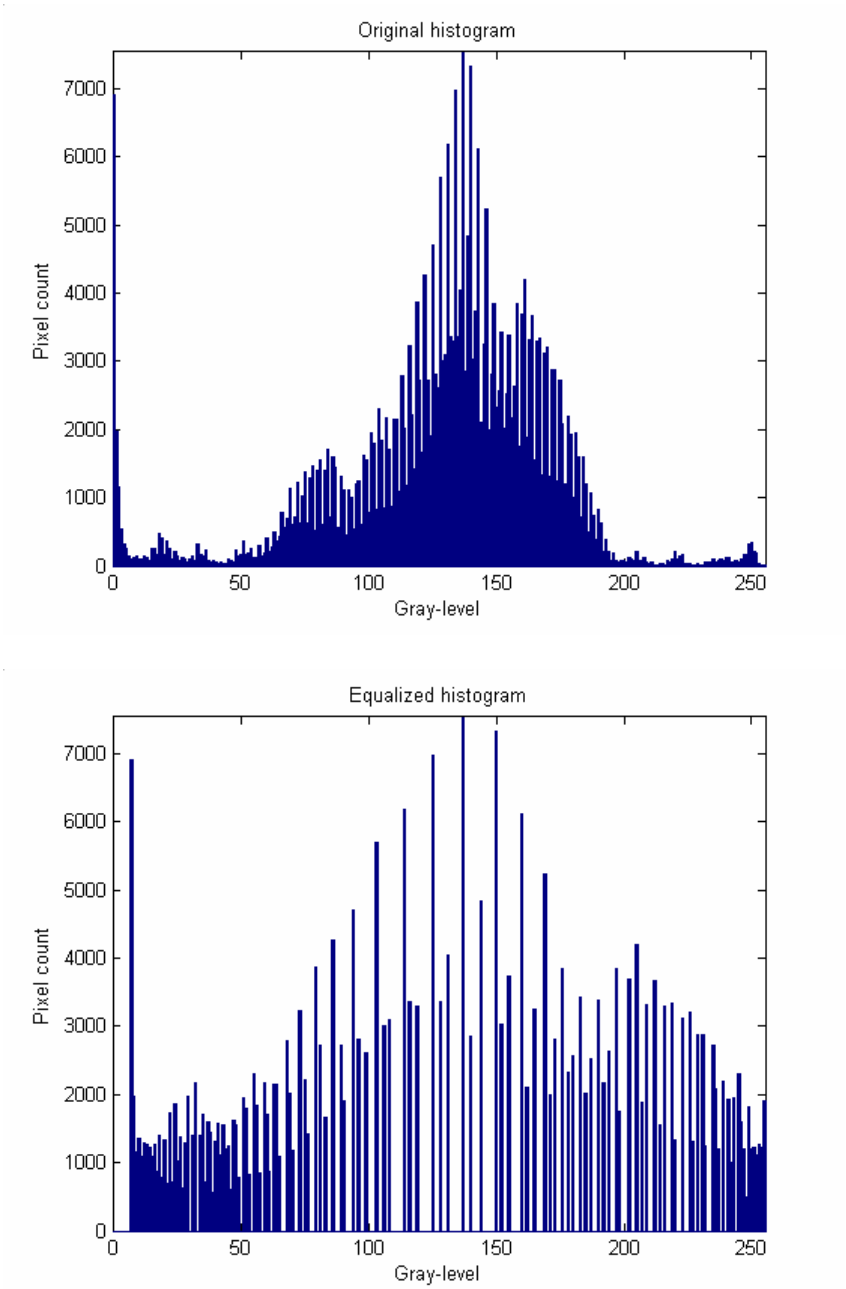

Figure 17: Image histograms before and after equalization.

Figure 16 and 17 show the histogram equalization results and corresponding histograms. The improvement over the original image is quite evident, as the treeline and foliages are now much more clearly defined. Looking at the histogram plots, the gray levels of the equalized image are spread out,

resulting in an increase in the dynamic range of gray levels and hence overall, contrast of the image.

Histogram equalization significantly improves the visual appearance of the image. Similar enhancement results could have been achieved by using a contrast stretching approach, but the main advantage of histogram equalization over manual contrast stretching or manipulation techniques is that the former is fully automatic, without the need to select any setting or to adapt to the original histogram distribution of the image.

F. ADAPTIVE HISTOGRAM EQUALIZATION

In low contrast images, the features of interest may occupy only a relatively narrow range of gray scale, with the majority of gray levels occupied by “uninteresting areas” such as background and noise. These “uninteresting areas” may also generate large counts of pixels and hence, large peaks in the histogram. In this case, the global histogram equalization amplifies the image noise and increases visual graininess or patchiness. The global histogram equalization technique does not adapt to local contrast requirements, and minor contrast differences can be entirely missed when the number of pixels falling in a particular gray range is small.

Adaptive Histogram Equalization (AHE) is a modified histogram equalization procedure that optimizes contrast enhancement based on local image data. The basic idea behind the scheme is to divide the image into a grid of rectangular contextual regions, and to apply a standard histogram equalization in each. The optimal number of contextual regions and the size of the regions depend on the type of input image, and the most commonly used region size is 8x8 (pixels). In addition, a bi-linear interpolation scheme is used to avoid discontinuity issues at the region boundaries.

Figure 18 illustrates the application of the interpolation scheme at the boundaries. Gray level assignment at the sample positions indicated by the white dot are derived from gray-value distributions in the surrounding contextual

regions. The points *A, B, C,* and *D* are the centers of the surrounding contextual regions; region-specific gray level mappings ($g_A(s)$, $g_B(s)$, $g_C(s)$ *and* $g_D(s)$) are based on the histogram equalization of the pixels contained. Thus, assuming that the original pixel intensity at the sample point is s, its new gray value s' is calculated by bilinear interpolation of the gray-level mappings that were calculated for each of the surrounding contextual regions:

$$s' = (1-y)((1-x)g_A(s) + xg_B(s))+y((1-x)g_C(s) + xg_D(s)), \quad (24)$$

where *x* and *y* are normalized distances with respect to the point A. This gray level interpolation is repeated over the entire image [Zuiderveld, 1994].

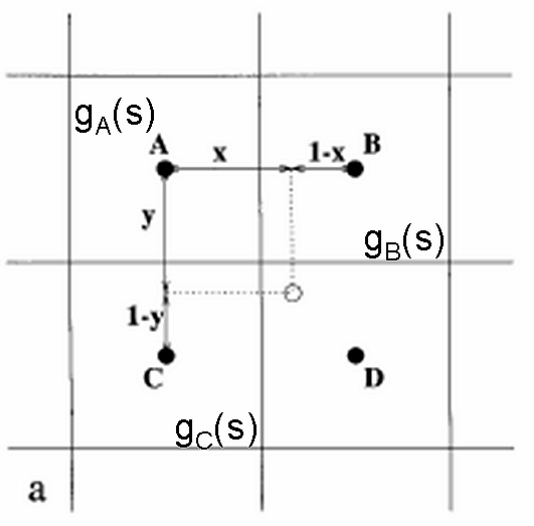

Figure 18: Bilinear interpolation to eliminate region boundaries [From Zuiderveld, 1994].

AHE is able to overcome the limitations of the standard equalization method as discussed earlier, and achieves a better presentation of information present in the image. However, AHE is unable to distinguish between noise and features in the local contextual regions. Hence, background noise is amplified in "flat" or "featureless" regions of the image, which is a major drawback of the method.

G. CONTRAST LIMITED ADAPTIVE HISTOGRAM EQUALIZATION

The noise problem associated with AHE can be reduced by limiting contrast enhancement specifically in homogeneous areas. These areas can be characterized by a high peak in the histogram associated with the contextual regions since many pixels fall inside the same gray level range. The Contrast Limited Adaptive Histogram Equalization (CLAHE) limits the slope associated with the gray level assignment scheme to prevent saturation, as illustrated in Figure 19. This process is accomplished by allowing only a maximum number of pixels in each of the bins associated with the local histograms. After “clipping” the histogram, the clipped pixels are equally redistributed over the whole histogram to keep the total histogram count identical. The CLAHE process is summarized in Table 1.

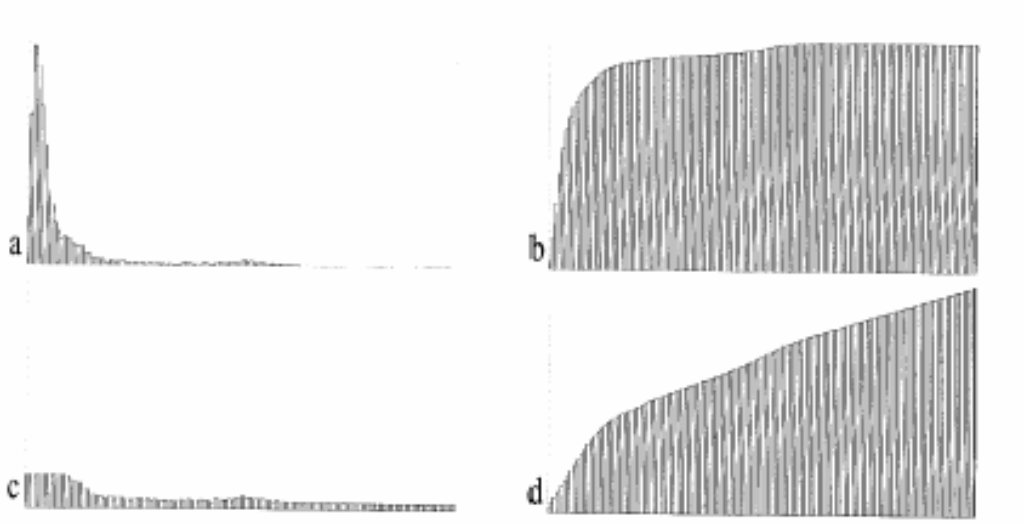

Figure 19: Principle of contrast limiting as used in CLAHE. (a) Histogram of a contextual region containing many background pixels. (b) Calculated cumulative histogram. (c) Clipped histogram with excess pixels redistributed throughout the histogram. (d) Cumulative clipped histogram with maximum slope set to the clip limit [From Zuiderveld, 1994].

The clip limit is defined as a multiple of the average histogram contents and is actually a contrast factor. Setting a very high clip limit basically limits the

clipping and the process becomes a standard AHE technique. A clip or contrast factor of one prohibits any contrast enhancement, preserving the original image.

Table 1. Summary of CLAHE process [Mathworks, 2003].

1. Obtain all the inputs: • Image • Number of regions in row and column directions • Number of bins for the histograms used in building image transform function (dynamic range) • Clip limit for contrast limiting (normalized from 0 to 1)
2. Pre-process the inputs: • Determine real clip limit from the normalized value. • If necessary, pad the image (to even size) before splitting into regions.
3. Process each contextual region (tile) thus producing gray level mappings: • Extract a single image region. • Make a histogram for this region using the specified number of bins. • Clip the histogram using clip limit. • Create a mapping (transformation function) for this region.
4. Interpolate gray level mappings in order to assemble final CLAHE image: • Extract cluster of four neighboring mapping functions. • Process image region partly overlapping each of the mapping tiles. • Extract a single pixel, apply four mappings to that pixel, and interpolate between the results to obtain the output pixel. • Repeat over entire image.

The CLAHE process and command can be found in the Image Processing Toolbox (version 4.1) of MATLAB (version 6.5, release 13).

The main advantages of the CLAHE transform are its modest computational requirements, ease of use and excellent results on most images. Figure 20 compares the CLAHE result to that obtained by the standard histogram equalization method. The CLAHE image has less amplified noise and avoids the brightness saturation in the standard histogram equalization. Additional comparison samples are included in Appendix B.

CLAHE does have its limitations. Since the method is aimed at optimizing contrast, there no direct 1-to-1 relationship between the gray values of the original image and the CLAHE processed result. Pixels of the same gray level in the original image may be mapped to different gray levels in the output image, because of the equalization process and bilinear interpolation. Consequently, CLAHE images are not suited for quantitative measurements that rely on physical meaning of image intensity [Zuiderveld, 1994].

Figure 20: Comparison of images obtained from standard histogram equalization (top image) and from CLAHE (bottom image). The CLAHE image has less amplified noise and avoids saturation by the bright source in the image. Figure 8 contains the original image.

THIS PAGE INTENTIONALLY LEFT BLANK

III. IMAGE ENHANCEMENT BY CLAHE

A. SPATIAL FREQUENCY

An image can be expressed in both the spatial and the frequency domains. The spatial domain is simply the two-dimensional image space which contains an array of pixels with intensity values representing the image. The image can be converted from the spatial domain to the frequency domain by Fourier transform.

The periodicity with which the image intensity values change is commonly referred to as the spatial frequency. The image value at each position (f_x, f_y) in the frequency domain represents the amount by which the intensity values in the image vary over a specific distance related to the spatial frequencies f_x and f_y (for a 2-dimensional image). For a simple image that is totally grey in color, i.e. one single gray value in all pixels, there will be no frequency component in both the x- and y-directions, although there will still be a zero frequency component corresponding to the single gray value of the image, or in other words, the DC component of the image. If there is a change in intensity or gray level values, there will be some frequency components along the direction of change in the frequency domain. There will be only one frequency component if the change is purely sinusoidal.

For example, suppose that there is the value 20 at the point that represents the frequency 0.1 (or 1 period every 10 pixels). This means that in the corresponding spatial domain, the intensity values vary from dark to light and back to dark over a distance of 10 pixels, and that the contrast between the lightest and darkest is 40 gray levels (2 times 20).

The significance and correlation of the spatial frequency to the image is illustrated in Figure 21. A simple square-in-square image is generated with different degrees of contrast against the background as shown. For the first image, the background is set at a gray level of 100 and the square at 128, while for the second image; the background is set at 0 (black) and the square at the

same level of 220. The corresponding spatial frequency spectra are plotted and the increased higher frequency components due to the increased contrast between object and background are clearly shown.

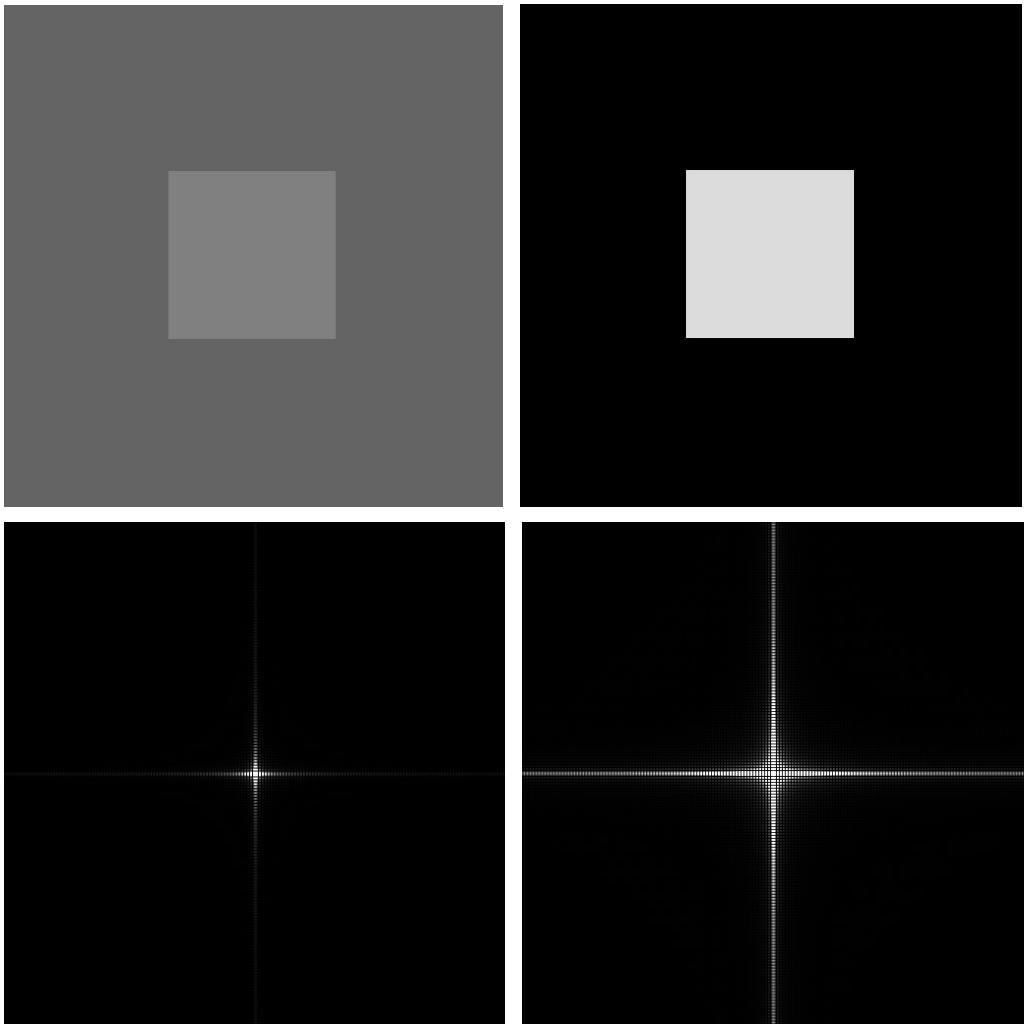

Figure 21: A simple image with its corresponding spatial frequency spectrum and the same image with a higher contrast between object and background, showing increased higher frequency components.

Hence, a high spatial frequency therefore represents a large change in intensity or contrast over short image distances. This can be translated to edges and sharp details in the image. The larger the amplitude or the frequency power, the greater the contrast change. The zero frequency in the frequency domain will correspond to the baseline intensity level in the image [HIPR, 2003].

To reinforce this point, the standard test image “Lenna” is used to illustrate the visual effect of boosting the higher spatial frequencies. The original gray-scale “Lenna” image (512x512) is converted to the frequency domain and components beyond the 150^{th} pixel (arbitrary chosen) away from the zero frequency are enhanced 250% in magnitude. The resulting image is shown on the right of Figure 22, which has sharper details (e.g. the lines of the hat). Hence, increasing the power of the higher frequency components enhances the edges and sharpens the details in the image, very much similar to a high-boost filter. The bottom pair of images in Figure 22 illustrates the effect of increasing the zero frequency component by 20% (the brightness of the image is increased).

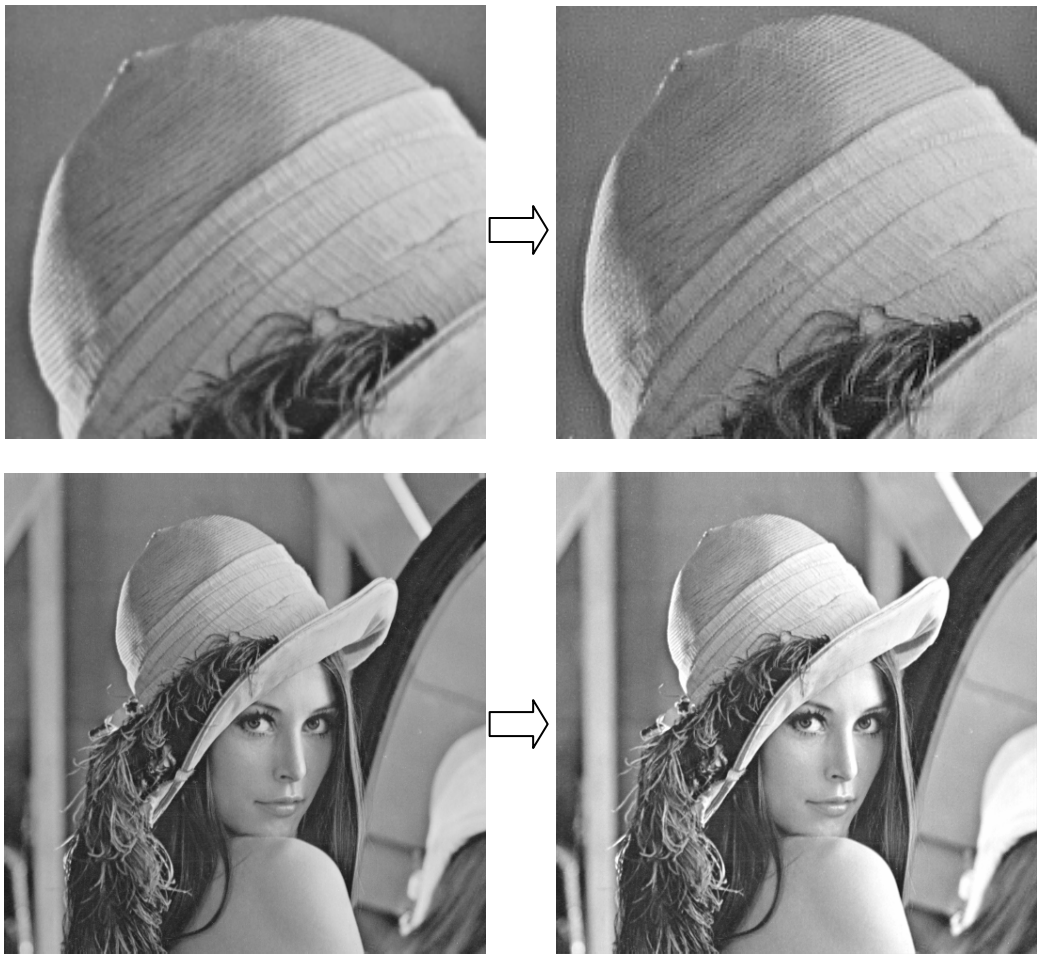

Figure 22: Effect of adjusting spatial frequency powers on the image. The top pair of images illustrates an increase in the power of the higher frequency components, while the bottom pair represents an increased power in the zero frequency component.

B. IMAGE QUALITY ASSESSMENT

The aim of image processing is naturally concerned with producing better images. But the key question is how do we quantify or measure the term “better” in image quality assessment. There is no absolute measuring scale like the kilogram in weight or the meter in distance. The fact remains that the image is ultimately perceived by a pair of human eyes and interpreted by the human brain for whatever purpose the image is intended for. Hence, the assessment of image quality is always subjective. There have been attempts to introduce an objective assessment methodology of image quality, such as mean-square error, probability of detection and peak signal-to-noise ratio [Barret, 1990]. But the basic difficulty is that images can be used for a variety of functions or purposes (e.g. classification, detection and measurement). A “good” image for one purpose may not be suitable for another. Furthermore, the performance of the human visual system (including the human brain) is not consistent even for the same image, let alone among individuals. Experience, eye-sight, training, age, physical conditions and fatigue will all affect the final interpretation of the image.

An image is always produced for a specific purpose or task, and the only meaningful measure of its quality is how well it fulfills that purpose. An objective approach to assessment of image quality must therefore start with a specification of the task and then determine quantitatively how well the task is performed or achieved [Barrett, 1990]. For example, in assessing the image quality for image compression, the mean-square error is a relevant and objective measure of the amount of distortion in the compressed image, as the smaller the error, the better the image. In the case of night vision images, their main purpose will be for detection of objects and providing information about the surrounding, when the human eyes are not sensitive enough under the low-illumination conditions. A quantitative measure for such a purpose would be the probability of detection or the time to detection. However, all the II and TI images used in this thesis are samples provided by the Naval Research Laboratory, as suitable imagers were not available at the time of the study. Some of the images contain identifiable objects, such as ships and fence, while others are just general outdoor scenes of

foliage. There is unfortunately no “hidden” object implanted in the scenes to measure quantitatively the quality of the image with respect to its purpose for detection.

Another objective measure of night vision images could be the number of edges or the intensity of the edges in the image. With more enhanced edges, more details and more information can be perceived from the image. As discussed in the previous section, edges in the image correspond to high spatial frequencies. Hence, for the same image, if there is more power in the higher spatial frequencies, the edges will be enhanced and hence, more details will be detectable. This is similar in principle to the highpass filter in the frequency domain as described in Chapter II. In this respect, the quality of the image can therefore be judged to be better, as the enhanced edges would improve the information content of the image, and the increased power in the high spatial frequencies can be measured objectively.

C. ANALYZSIS OF ENHANCEMENT RESULTS

A CLAHE-processed night vision image is compared to its original unprocessed version in Figure 23. The CLAHE processed image appears to have “better clarity” as image edges and details have been enhanced by the CLAHE process. The profile of the foliage and the river bank are “easier” to identify. The single small tree in the center of the image is a good example of enhancement produced by CLAHE. Therefore, this edge enhancement would theoretically be accompanied by increased higher spatial frequency components in the frequency domain of the image. Our aim is to compare the frequency spectra of the original and the processed image for increased higher frequencies and to use this difference as an objective basis for judging improvement in image quality, instead of relying solely on subjective visual assessment.

Figure 23: Unprocessed (top) and CLAHE processed night vision images (bottom) for comparing the improvement in image contrast and details enhancement by CLAHE.

1. Spatial Frequency Spectrum

The image is first converted from the spatial domain to the frequency domain by using the 2-dimensional discrete Fast Fourier Transform (FFT) in MATLAB. The image is "padded" (to 1024x1024) during the FFT process, i.e. adding zeros to the beginning and/or end of the time-domain sequence. This addition increases the frequency resolution of the FFT and does not affect the frequency spectrum of the image. As the image sizes are 480x640, padding the image to even dimensions of power 2 (2^{10} = 1024) also reduces the FFT computation time. The Fourier transform is also shifted to center the zero frequency with respect to the image center. The frequency power spectrum is then plotted out using the "mesh" command in MATLAB.

Figure 24 plots the frequency responses of the unprocessed and the corresponding CLAHE-processed image shown in Figure 23. Clearly, there is an increased amount of higher frequency components, as shown by the higher spikes and color-coded profiles contained in the pictures, i.e. there is more power in the higher spatial frequencies. This observation supports the fact that the edges have been enhanced. Notice that the zero frequency is centered at the location (512,512) as a result of the padding to 1024x1024.

2. Spectrum Power Distribution

Next, the cumulative power distribution with respect to the distance from the center zero frequency (in terms of number of pixel count) is plotted to further examine the frequency power distribution. This computation is accomplished by superimposing a square window over the frequency spectrum and summing the power contained within it. The center of the square will overlie the zero frequency center and the distance will be equivalent to half the length of the square window. A contour plot of the frequency spectrum was created with MATLAB to illustrate the expanding window for computing the total amount of power, as shown in Figure 25. The contour plots also provide a different viewing aspect for comparing the frequency spectra of the processed and unprocessed images.

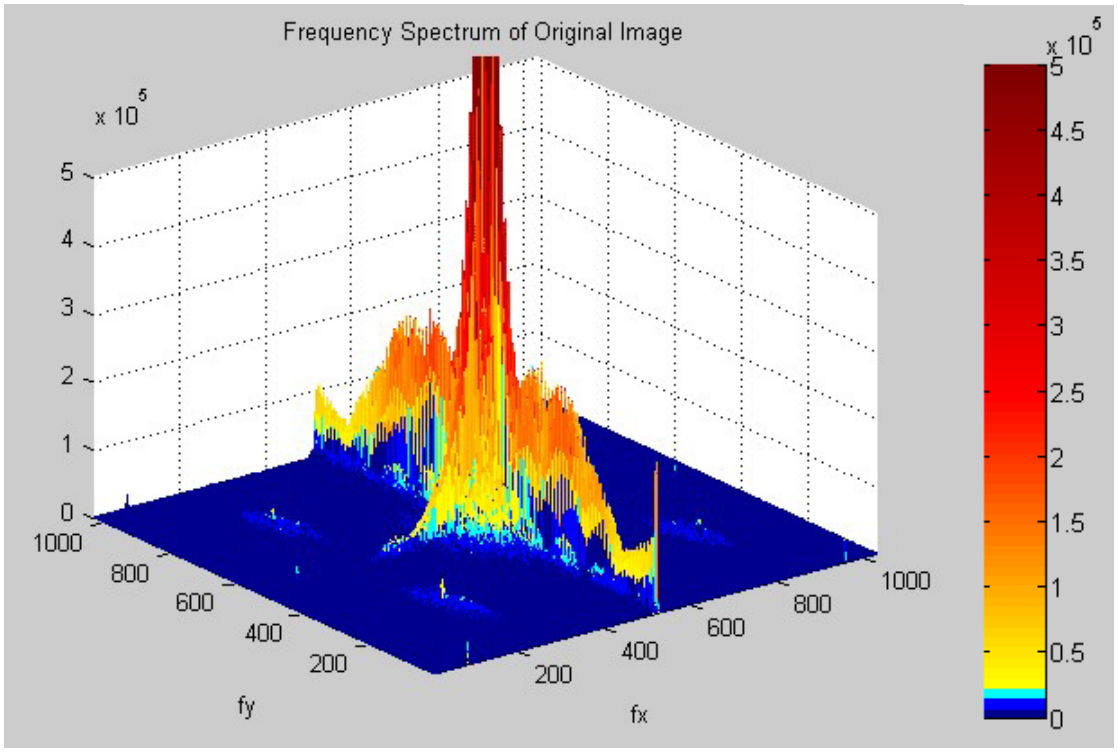

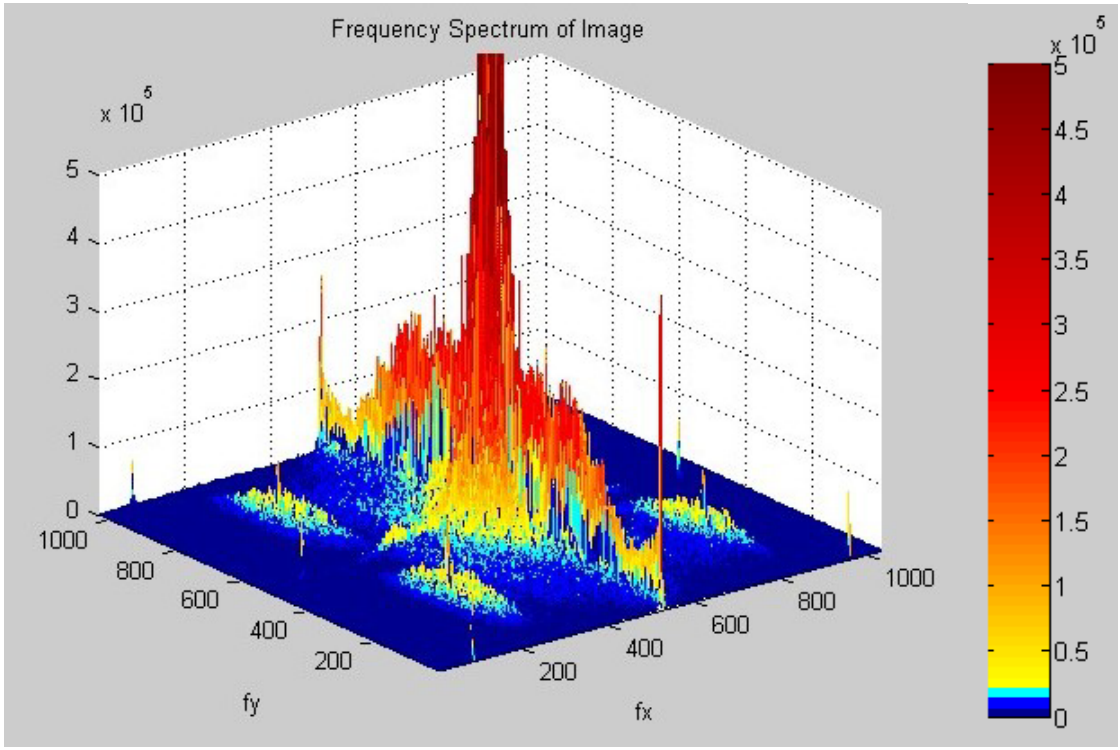

Figure 24: Frequency spectrum plot of the unprocessed image and the CLAHE processed image, showing an increase in the power of higher frequency components. The maximum peak value is clipped at $5x10^5$ to focus on the power distribution beyond the zero frequency.

.

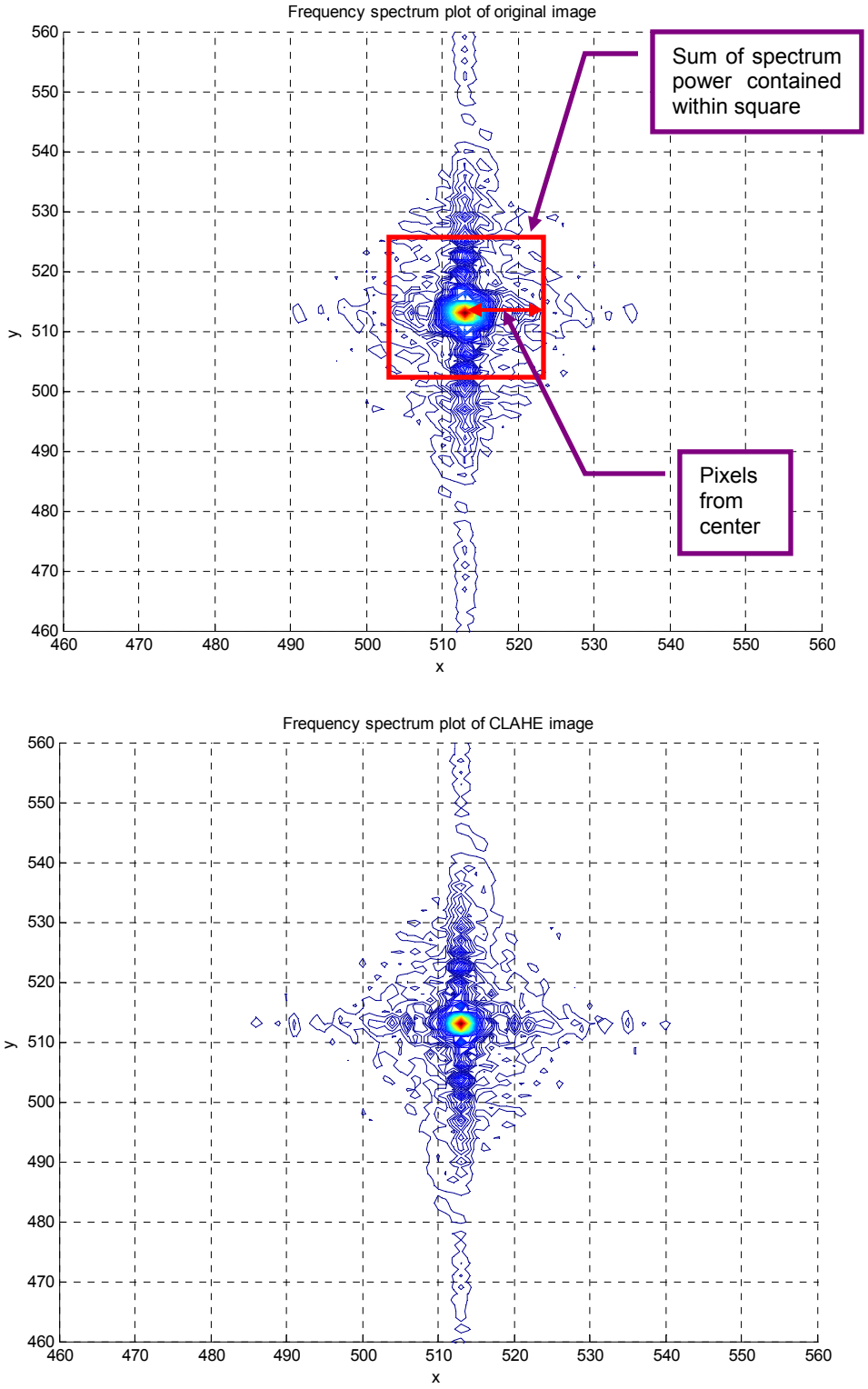

Figure 25: Contour plots of the unprocessed image and the CLAHE processed image. The summation process to compute the power distribution is as illustrated on the top image.

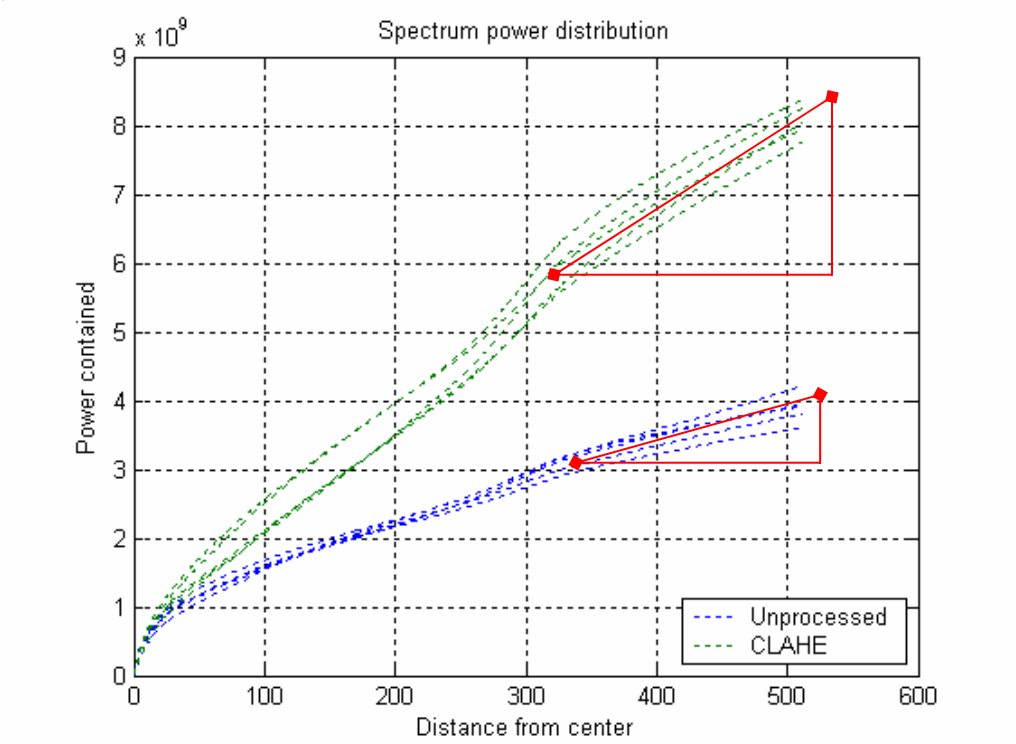

Figure 26: Cumulative spectrum power distribution plots for six pairs of images, showing an overall increased in total spectrum power and a higher percentage of power in the higher frequencies.

The cumulative spectrum power distributions of the original and processed images are plotted in Figure 25. A total of six image pairs were used to give an indicative trend of the distribution profile. Figure 25 shows that the total spectrum power has been increased by the CLAHE process, which can be translated here to increased brightness and contrast in the image. The rate of increase in the cumulative power in the second half of the curves, i.e. the higher frequencies, is also steeper for the CLAHE-processed images (the green dotted lines) than that of the original image, as illustrated by the gradient triangles in red. This difference implies that there is a higher percentage of power contained in the higher frequencies and indicates edge enhancement in the processed images.

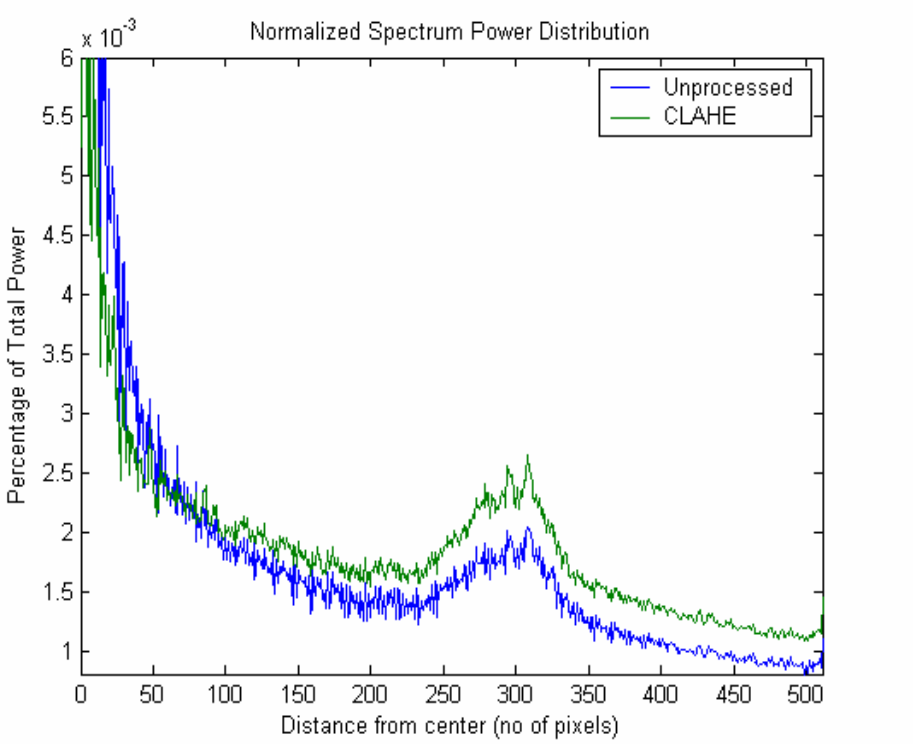

Figure 27: Spectrum power distribution plot. The percentage of power contained in the higher frequencies is higher for the CLAHE-processed image as shown by the green profile.

Figure 27 shows that a higher percentage of power is contained in the higher frequencies (from the 100th pixel onwards for this image) in the CLAHE processed image than in the original unprocessed image. We also note that the percentage of power in the lower frequencies is lower for the processed image, which is not significant as the vital information, i.e. the edge content, is contained in the higher boosted frequencies.

In summary, the results presented in Figure 26 and 27 validate the observation that the CLAHE process has enhanced the image edges and details, as evident from the boosted higher spatial frequency components. The CLAHE-enhanced images are therefore judged to be improved.

3. Histogram

The histogram of the CLAHE-processed image is compared with its unprocessed version in Figure 27. The CLAHE processed image has a more evenly-distributed and wider spread of the gray levels, which translates to an image with better contrast as seen in the processed image in Figure 22. Since the amplitude of spatial frequency is dependent on the degree of contrast change, a larger contrast range in the histogram is therefore linked to increased spatial frequency components.

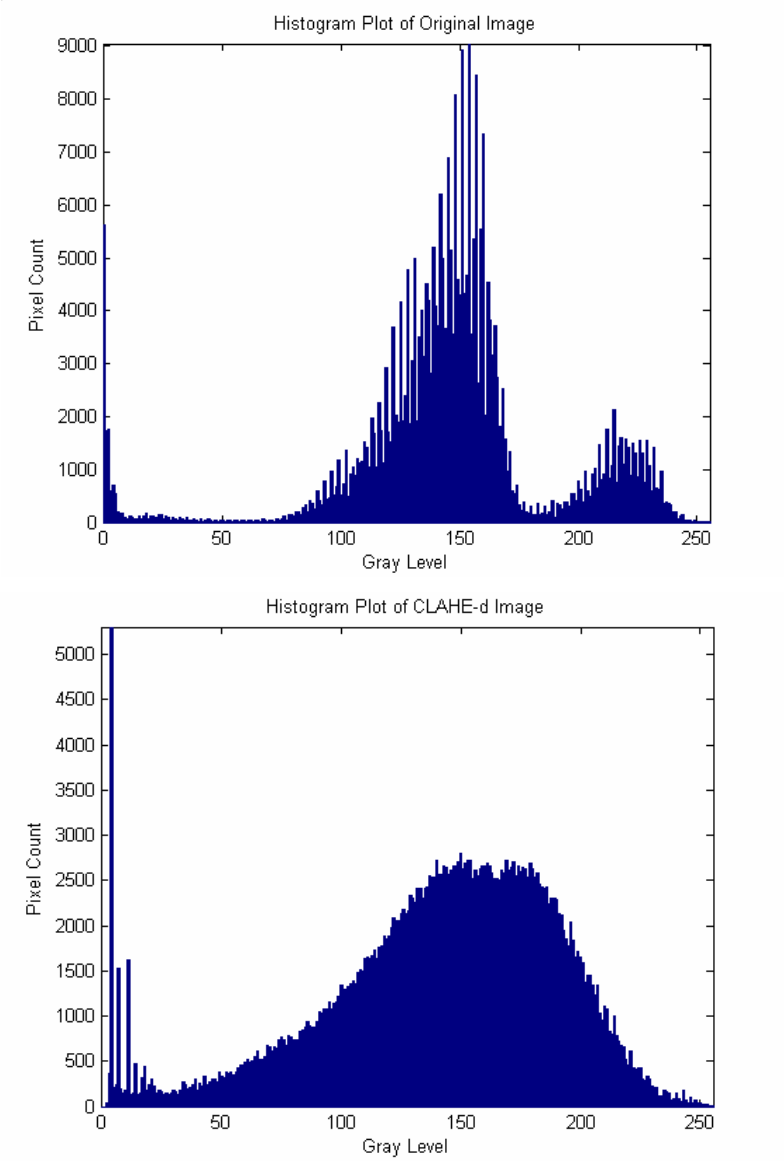

Figure 28: Comparison of the histograms of the unprocessed and the CLAHE processed image. The images are from Figure 22.

D. SUBJECTIVE ASSESSMENT

The eventual user of an image is still the human being. Theoretical figures of merit and engineering computations may be inadequate in predicting the human response. Hence, any image quality assessment should still be validated by human subjects for acceptance.

1. Test Outline

A subjective test was conducted to evaluate the image enhancement by CLAHE. Fifteen students from the Naval Postgraduate school, aged 28 to 38 years old, were approached for the test. Fifteen is the recommended minimum number of test subjects by the International Telecommunication Union [ITU-R BT.500-11, 2002]. All subjects were voluntary and signed informed consents. Five of the subjects have no prior experience with night vision images or night vision devices, while the rest have experience with either the night vision goggle or the Thermal Imager.

20 image pairs consisting of one CLAHE-processed and one unprocessed image of the same scene, were presented to the subjects on a Toshiba TECRA 9100® laptop with 32-bit color and 1024x768 resolution setting. Brightness setting of the laptop LCD was at 50% and the test was conducted in a dimly-lighted room. Subjects were shown two consecutive sequences of the same image pair and asked to indicate their preference as to which one of the two images conveyed the most information or details about the scene. “Most information” can be interpreted as what allows the subject to see more objects (if any) or provides a better situation awareness about the scene. A choice of “neutral” can be entered when the subject finds that both images are comparable or there is no significant difference between the two. The display timing of the image sequence was set as: three seconds (image 1), one second (blank screen), three seconds (image 2), followed by a two seconds pause before the same sequence was repeated for a second time. Each test lasted approximately 15 minutes.

The order of the processed and unprocessed image in the display sequence was randomized. Of the 20 image pairs, 5 were thermal images while the rest were NVD or II images. The thermal image pairs were interspersed among the II image pairs randomly. Due to the inherent high contrast present in these thermal images, it is expected that the enhancement by the CLAHE process would be insignificant and may even degrade the image quality. Therefore, the thermal images were inserted to break any monotony of choice that may arise in the experiment.

2. Results

Survey results are summarized in Table 2. 75% of the subjects found the CLAHE-processed night vision images to be more informative and a more meaningful representation of the scene, as compared to the original associated unprocessed images. This finding supports the proposition that the content of the image has been enhanced by the CLAHE process.

The majority of the subjects did not find the CLAHE-processed thermal images to be better in providing information. About only 35% of the subjects found the processed thermal images to be more effective in providing information. This result could be due to the fact that the thermal images provided by NRL already have very good original contrast and as a result, the contrast enhancement by CLAHE is not significant. In some cases, the subjects commented that the image was “over-contrasted”, making the image “unnatural” and details difficult to identify. An example is shown in Figure 28. The image pair in Figure 28 is actually image pair number 10 in the subjective test, which received the lowest score.

The CLAHE process enhancement is effective on the low-contrast night vision images as validated in the subjective testing. Thermal images generally have better contrast due to suppression of the background by AC coupling during the filtering process. But there would still be cases of low contrast thermal images, such as during dusk and dawn when the background temperature draws near the object temperature due to difference in thermal conductivity of object

and background. Therefore, the CLAHE process is still applicable to thermal imagery.

Table 2. Subjective Test Results

		Image Preference (% of subjects)			
Image Pair	Type	Processed		Unprocessed	Neutral
1	II	80.0		13.3	6.7
2	II	73.3		26.7	-
3	II	93.3		-	6.7
4	II	66.7		26.7	6.7
5	TI		26.7	66.7	6.7
6	II	53.3		33.3	13.3
7	II	60.0		20.0	20.0
8	II	60.0		26.7	13.3
9	II	86.7		13.3	-
10	TI		20.0	66.7	13.3
11	II	80.0		20.0	-
12	TI		46.7	53.3	-
13	II	80.0		13.3	6.7
14	II	60.0		20.0	20.0
15	TI		46.7	40.0	13.3
16	II	80.0		13.3	6.7
17	II	86.7		13.3	-
18	TI		33.3	60.0	6.7
19	II	80.0		6.7	13.3
20	II	86.7		6.7	6.7
Average preference for CLAHE-processed II image					**75.1**
Average preference for CLAHE-processed TI image					**34.7**

Figure 29: Unprocessed and processed thermal image pair, illustrating the minimal improvement by the CLAHE process.

3. Observations and Comments

a. No Objectivity in Images

Most of the images obtained from the Naval Research Laboratory are outdoor scenes with no particular object for detection. The general feedback from the subjects is that it is difficult to judge the information content of the image without a specific object to look out for, i.e. some specific detail that could be seen in only the enhanced image and not the original image. Images which have such characteristics would aid in making the test more objective. A few of the subjects entered a “neutral” choice, basically because they could see the same amount of details in both original and enhanced images as both sets of images contained the same information, even though the processed images appeared clearer. This explains the relative lower score for image pairs 6, 7, 8 and 14 (the images are available in Appendix B).

Hence, for future subjective testing, image pairs should be created (when the actual hardware is available) with one or more objects for detection. The objects could be obscured by low-light or camouflage to reduce their contrast and visibility in the original night vision images. These objects would be easier to see and detect after the CLAHE enhancement. A good example is the image pair from Figure 8 (original) and Figure 20 (CLAHE-processed). More ships can actually be seen with the enhancement, as agreed by 86.7% of the subjects.

b. Scanning versus Staring

Some of the subjects found the display time for the images to be too short for a proper assessment, which relates directly to the issue of scanning or staring assessment. Scanning is more concerned with wide-area surveillance where the assessment time is short and the images are displayed real-time; for staring, the image display is static. The commonality linking the two is the time to detection. Subjects would be likely to take less time to detect an object when the image has better contrast. Hence, the time to detection could be another objective measure of the image quality. However this measure can only be explored when there is object implanted in the image, as discussed in the previous section.

c. Experience Factor

Five of the fifteen subjects did not have any prior experience of viewing night vision images or devices. Separating the two groups of subjects, the percentage for the CLAHE-processed image went up to 78% for those subjects with night vision experience as shown in Table 3, and the percentage is only 69% for subjects without any prior experience as per Table 4. The subjects from the group “without experience” indicated that they found enhanced noise and “graininess” in the CLAHE-processed image to be distracting, and preferred the original unprocessed image. The noise in question is actually inherited from the original image and hardware, something that experienced subjects have already accepted as a general characteristic of night vision images. Therefore, experience turns out to be a factor in the test results and should not be overlooked, as this group represents the new-users of night vision devices. It is also noted that there were more “neutral” choices from the experienced subjects, which could be explained by the lack of objectivity in the test images as discussed earlier.

We recommend that the number of subjects be increased and include an equal number of experienced and inexperienced viewers for future studies. This would allow a more accurate analysis of the acceptance of the CLAHE enhancement and the influence of experience. The larger subject base would also better represent the population of users of night vision and thermal devices.

d. Original Image Quality

Image pair 4 received a relatively lower score for an II image. Examining the image pair reveals that the original image has reasonably good contrast due to a light source in the sky. Hence, the enhancement by CLAHE was not significant, which is similar to the thermal image pairs where the most common response was a preference for the original image. Therefore, the CLAHE enhancement may not be always necessary.

Table 3. Subjective Test Results (with night vision experience)

		Image Preference (% of subjects)			
Image Pair	Type	Processed		Unprocessed	Neutral
1	II	90.0		10.0	-
2	II	90.0		10.0	-
3	II	90.0		-	10.0
4	II	70.0		20.0	10.0
5	TI		20.0	70.0	10.0
6	II	50.0		30.0	20.0
7	II	60.0		10.0	30.0
8	II	50.0		30.0	20.0
9	II	90.0		10.0	-
10	TI		20.0	70.0	10.0
11	II	90.0		10.0	-
12	TI		40.0	60.0	-
13	II	80.0		10.0	10.0
14	II	60.0		10.0	30.0
15	TI		50.0	40.0	10.0
16	II	90.0		-	10.0
17	II	90.0		10.0	-
18	TI		20.0	70.0	10.0
19	II	80.0		-	20.0
20	II	90.0		-	10.0
Average preference for CLAHE-processed II image					**78.0**
Average preference for CLAHE-processed TI image					**30.0**

Table 4. Subjective Test Results (without prior experience)

		Image Preference (% of subjects)			
Image Pair	Type	Processed		Unprocessed	Neutral
1	II	60.0		20.0	20.0
2	II	40.0		60.0	-
3	II	100.0		-	-
4	II	60.0		40.0	-
5	TI		40.0	60.0	-
6	II	60.0		40.0	-
7	II	60.0		40.0	-
8	II	80.0		20.0	-
9	II	80.0		20.0	-
10	TI		20.0	60.0	20.0
11	II	60.0		40.0	-
12	TI		60.0		-
13	II	80.0		20.0	-
14	II	60.0		40.0	-
15	TI		40.0	40.0	20.0
16	II	60.0		40.0	-
17	II	80.0		20.0	-
18	TI		60.0	40.0	-
19	II	80.0		20.0	-
20	II	80.0		20.0	-
Average preference for CLAHE-processed II image					**69.3**
Average preference for CLAHE-processed TI image					**44.0**

IV. CONCLUSIONS AND RECOMMENDATIONS

A. SUMMARY

The CLAHE algorithm is a digital contrast enhancement technique that emphasizes local details in the image while limiting noise amplification. This process is achieved with local histogram equalization and clipping, followed by bilinear interpolation.

CLAHE contrast enhancement has been found to be visually significant, and object detection is improved with the higher contrast in the images. Examining the frequency response of the enhanced image reveals increases in the higher spatial frequencies. As higher spatial frequencies correspond to edges in the image, the increase in power represents an enhancement of the edges and hence, an increase in visible image details. We also conducted a subjective testing where the majority of the human subjects indicated that the CLAHE-enhanced images were more informative than the original images.

Results indicated that the CLAHE process is effective in enhancing low-contrast images. However, the improvement is limited for images with initially good contrast, such as the thermal images in this study. Nevertheless, TI can still suffer from low-contrast during the day, especially during dusk and dawn. Therefore, the CLAHE enhancement scheme is still applicable to both night vision devices (Image Intensifiers) and Thermal Imagers. This enhancement would be attractive for Image Intensifiers since they are cheaper and more compact, and their main handicap is their low-contrast imagery.

The CLAHE process can be implemented in the form of a computer algorithm or a hardware electronic chip in the interface between the sensor and display. No modification is required on the sensor itself. The enhancement can also be real-time, as the CLAHE processing is not demanding. There is still a need for an on/off switch or option for the process as not all subjects found the enhancement beneficial at all times.

B. RECOMMENDATION FOR FURTHER RESEARCH

1. Subjective Test with Object Detection

A new set of matching night vision and thermal images containing specific objects should be created. The objects should be on the threshold of visibility in the unprocessed image and they should become detectable after the CLAHE enhancement. These image pairs can then be used in a larger or more extensive subjective test to determine the time to detection for these objects. Such test would help quantify the CLAHE improvement more objectively, and potentially justify its implementation cost.

2. Image Fusion

CLAHE-enhanced night vision images can be fused with their thermal counterparts (with or without enhancement) to assess any further improvement in image quality using the same frequency evaluation and subjective testing. One potential fusion algorithm to consider could be the nonlinear method proposed by Scrofani et. al. earlier (1997).

APPENDIX A: MATLAB ALGORITHMS

This Appendix contains the following MATLAB source files:

1. Histogram equalization (Test8_hist_equal.m).
2. Frequency spectrum plot (Test13_power.m).

```
% Test8_hist_equal.m
% Histogram equalization
% ==========================
% The input to the file has to be made manually in the m-file and run.
% The output will consist of four histogram plots, the original image
% and the processed image.
% ==========================

Aii = imread('21-I.tif');                % Input test image 21-I.tif

Aorg = Aii;
graylvl = 256;  % note the need to specify gray levels, typically it is 256
lvl = graylvl - 1;

disp('Generating histogram.....');
% ===== Generate histogram count =====
for k = 1:graylvl
   n_count(k) = length(find(Aii == k-1));
end

r = [0:1:lvl];                           % graylevels from 0 to 255
r_norm = r./lvl;                         % normalized
total = sum(n_count);                    % total pixels count
pdf = n_count./total;                    % generate probability distribution

s_cdf = pdf;                             % generate cumulative density function
for a = 1:length(r)-1
   s_cdf(a+1) = s_cdf(a+1)+ s_cdf(a);
end

s_int = s_cdf.*lvl;                      % rescale back to graylevel values
s_lvl = uint8(s_int+1.5);                % convert to integer by removing decimals
s_new = zeros(size(n_count));    % +1 to account for zero graylevel at 1st
column

disp('Equalising.....');
% ===== Combine count for same gray levels after transformation =====
for count = 1:1:lvl+1
   s_new(s_lvl(count)) = s_new(s_lvl(count))+ n_count(count);
end
s_new = s_new./total;                    % normalized new values

% ===== Remap graylevels in image =====
for m = 1:480
   for n = 1:640
   Aii(m,n) = s_lvl(double(Aii(m,n))+1);
```

```
    end
end

disp('Transforming image.....');

% ===== Counter-check graylevel transformation for equalization =====
for k = 1:graylvl
    n_check(k) = length(find(Aii == k-1));
end
disp('....done.');

% ===== Plot histograms =====
Figure(1)
subplot(2,2,1),bar(r,n_count),title('Original histogram'),axis tight;
subplot(2,2,2),bar(r_norm,s_cdf),title('Cdf'),axis tight;
subplot(2,2,3),bar(r_norm,s_new),title('Equalized histogram'),axis tight;
subplot(2,2,4),bar(r,n_check), title('Equalized histogram 2'),axis tight;
% the 3rd histogram is normalized and serve as a counter-check for the 4th
histogram

Figure(2)
imshow(uint8(Aorg), 256);
title('Original image')

Figure(3)
imshow(uint8(Aii),256);
title('Resultant image')

% ===== end =====
```

```
% Test13_power.m
% Plot the spectrum power distribution
% ============================
% The input to the file has to be made manually in the m-file and run.
% Input A is the original image while input B is the CLAHE processed image.
% The first figure output will be the cumulative spectrum power plot.
% The second figure output is the spectrum power distribution.
% ============================

clear;
Aii = imread('25-I.tif');              % input original image
Bii = imread('25-Iah.tif');            % input CLAHE image

Afft = fft2(Aii,1024,1024);            % fast fourier transform with padding
Afft2 = fftshift(Afft);                % center zero frequency
A2 = abs(Afft2);                       % take magnitude of complex

Bfft = fft2(Bii,1024,1024);            % fast fourier transform with padding
Bfft2 = fftshift(Bfft);                % center zero frequency
B2 = abs(Bfft2);                       % take magnitude of complex

% find center of spectrum
[n1 x] = max(max(A2,[],1));
[m1 y] = max(max(A2,[],2));

A_total = sum(sum(A2));
[m n] = size(A2);
dim_max = m - y;                       % find max dimensions of image
A_array(1) = A2(x,y);
A_arrayc(1) = A2(x,y);

% expanding square and sum
for dim = 1:dim_max
   A_arrayc(dim+1) = 0;
   for a = x-dim:x+dim
      for b = y-dim:y+dim
         A_arrayc(dim+1) = A_arrayc(dim+1)+A2(b,a);
         A_array(dim+1) = A_arrayc(dim+1)- A_arrayc(dim);
      end
   end
end

% find center of spectrum for CLAHE image
[n1b xb] = max(max(B2,[],1));
[m1b yb] = max(max(B2,[],2));
```

```
B_total = sum(sum(B2));
[mb nb] = size(B2);
dim_maxb = mb - yb;
B_array(1) = B2(xb,yb);
B_arrayc(1) = B2(xb,yb);

for dimb = 1:dim_maxb
   B_arrayc(dimb+1) = 0;
   for a = xb-dimb:xb+dimb
      for b = yb-dimb:yb+dimb
         B_arrayc(dimb+1) = B_arrayc(dimb+1)+B2(b,a);
         B_array(dimb+1) = B_arrayc(dimb+1)- B_arrayc(dimb);
      end
   end
end

% === Plot cumulative spectrum power distribution ===
figure;
plot(0:511,A_arrayc./A_total,0:511,B_arrayc./B_total)

% === Plot power distribution ===
figure;
plot(0:511,A_array./A_total,0:511,B_array./B_total)
% May have to zoom in the y aixs for a better view of the distribution

% ==== end =====
```

THIS PAGE INTENTIONALLY LEFT BLANK

APPENDIX B: CLAHE ENHANCED IMAGES

The following images are results obtained from using the Contrast Limited Adaptive Histogram Equalization (CLAHE) enhancement algorithm. The images on the left column are the original unprocessed night vision images, while the images on the right are the CLAHE processed images. These image pairs are used in the subjective testing to assess the improvement by the CLAHE method. The numbering of the image pair is the same as that used in the subjective test.

Original CLAHE

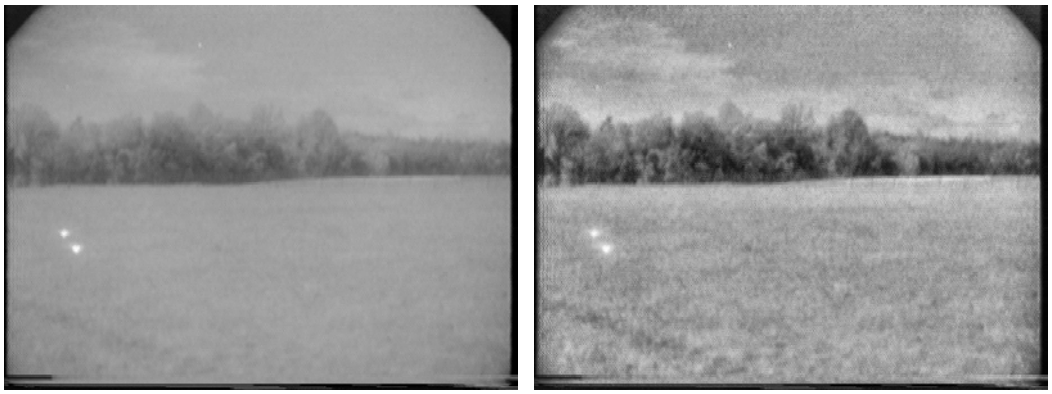

Image pair 1

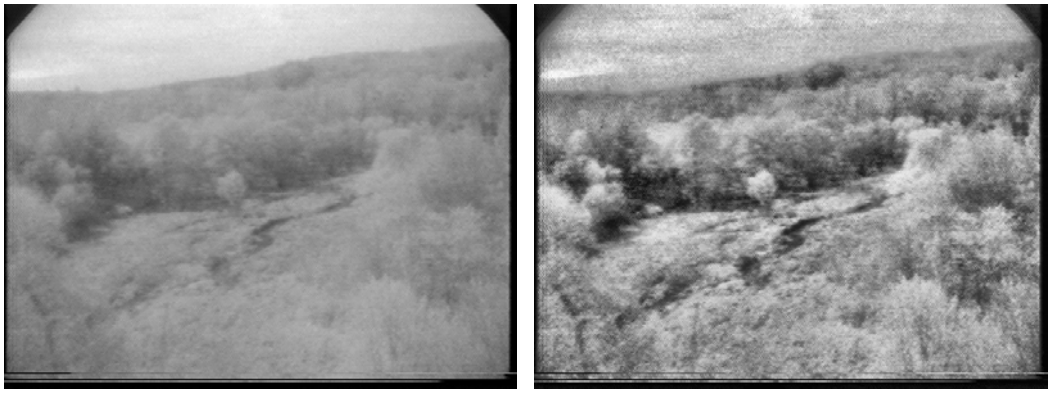

Image pair 2

Original CLAHE

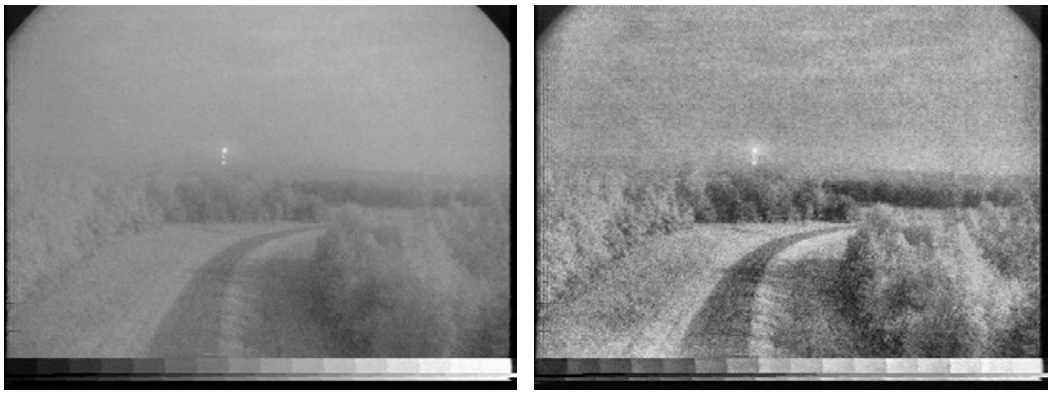

Image pair 3

Image pair 4

Image pair 5

Original CLAHE

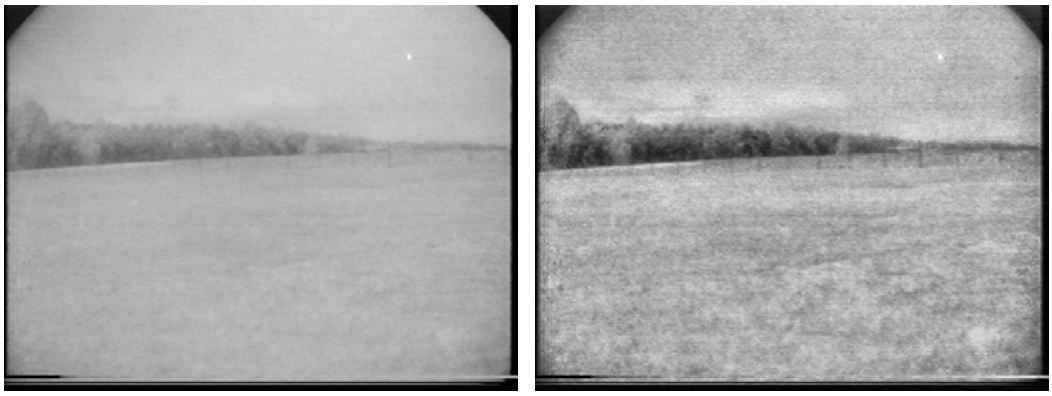

Image pair 6

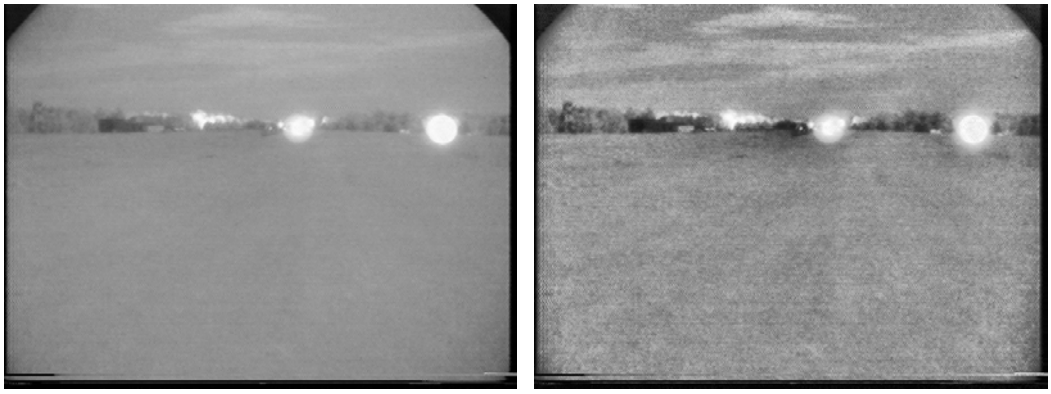

Image pair 7

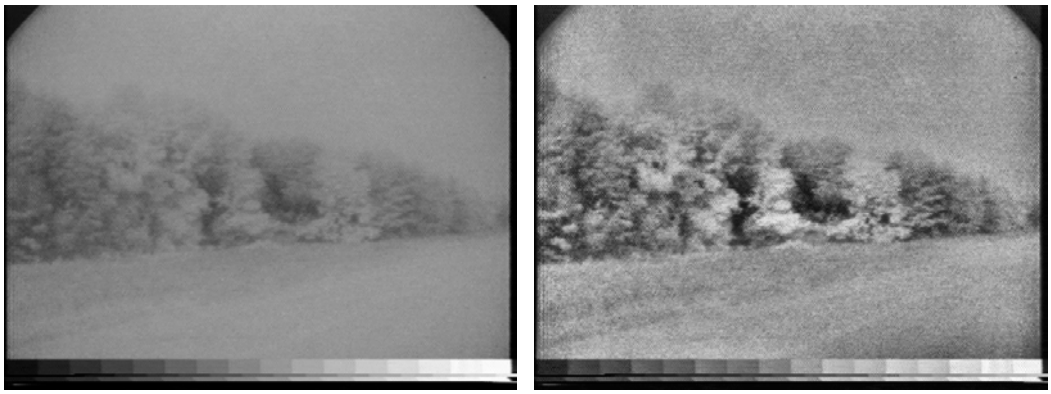

Image pair 8

Original CLAHE

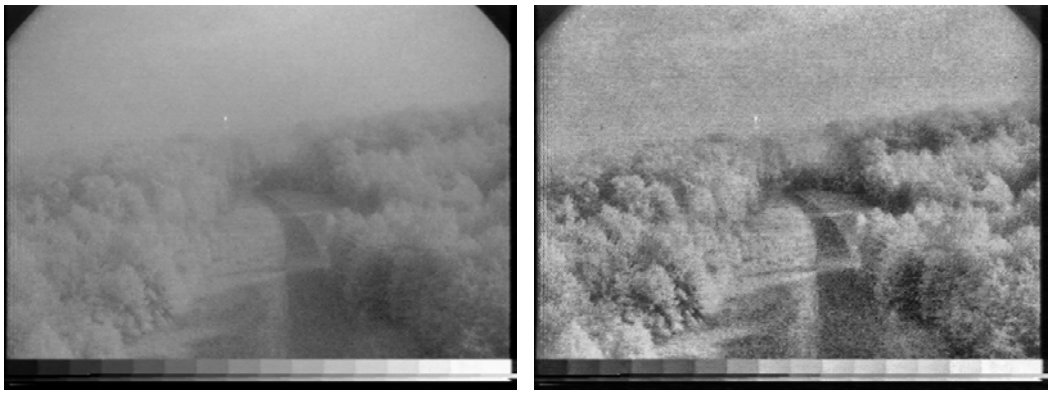

Image pair 9

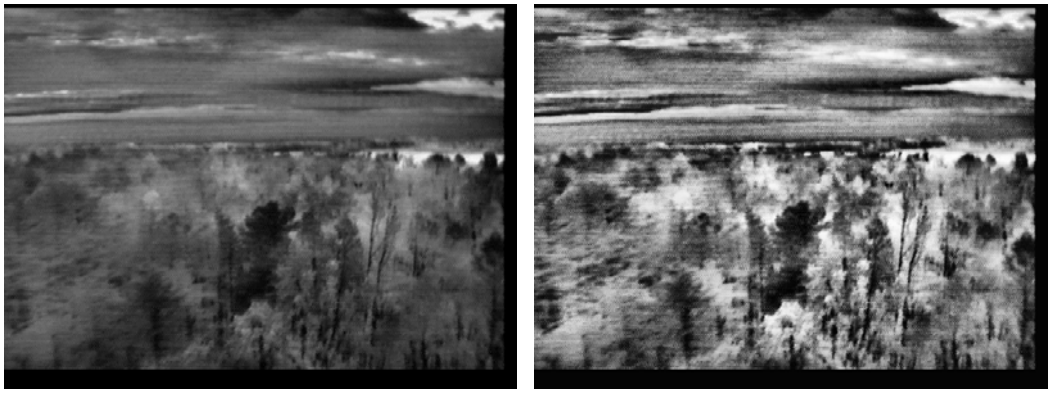

Image pair 10

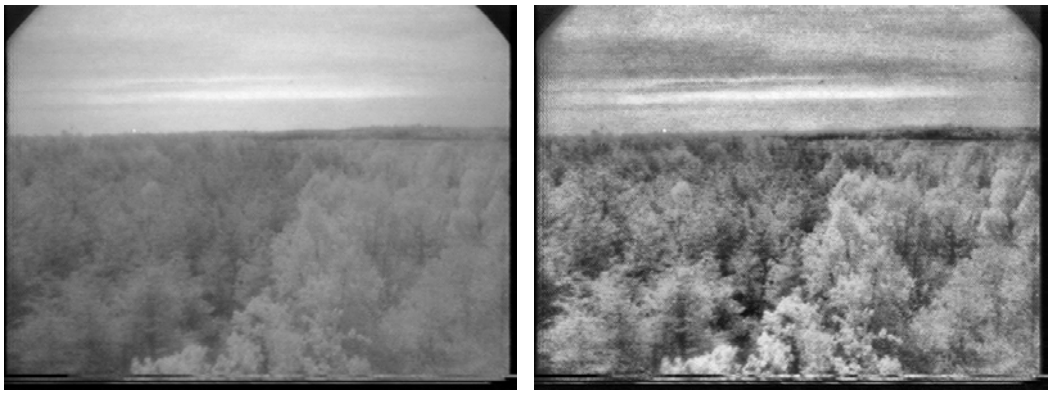

Image pair 11

Original CLAHE

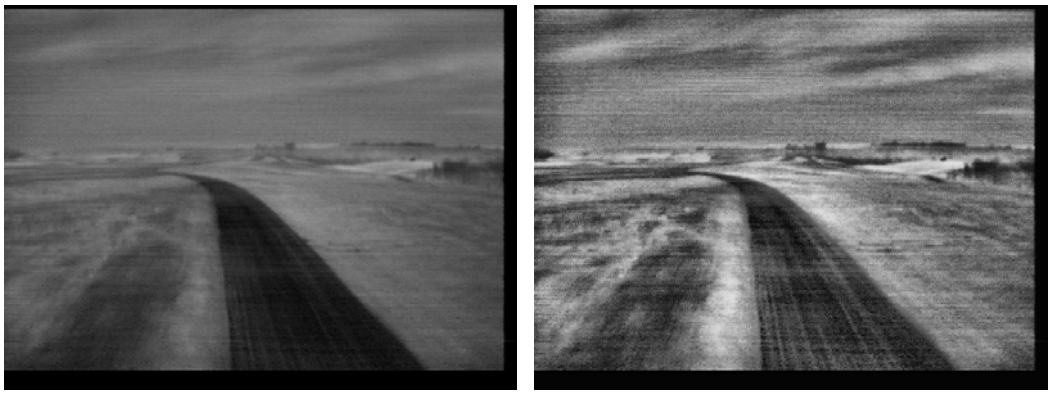

Image pair 12

Image pair 13

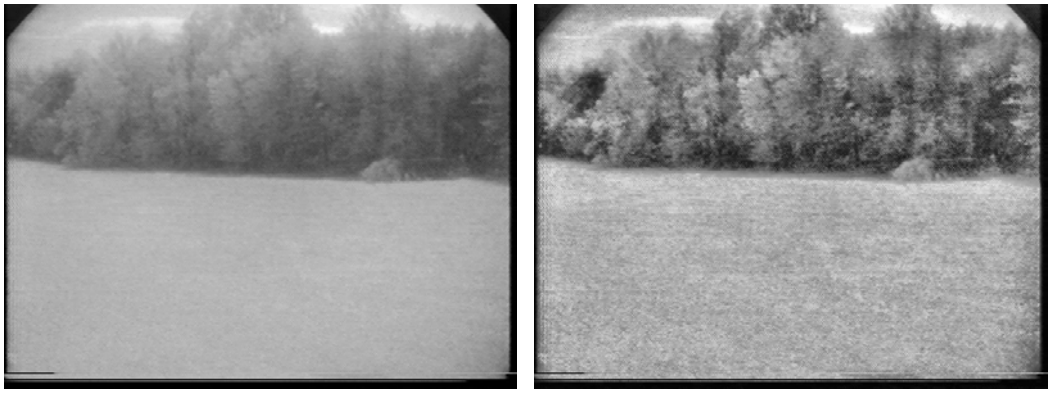

Image pair 14

Original CLAHE

Image pair 15

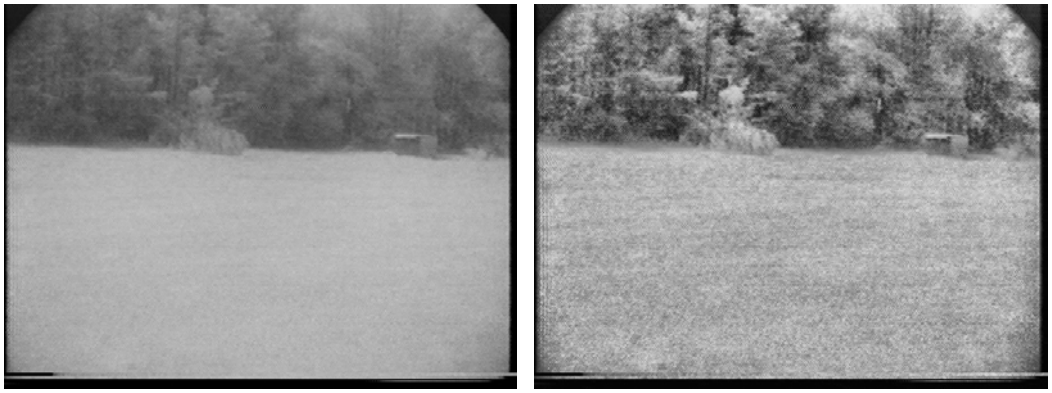

Image pair 16

Image pair 17

Original CLAHE

Image pair 18

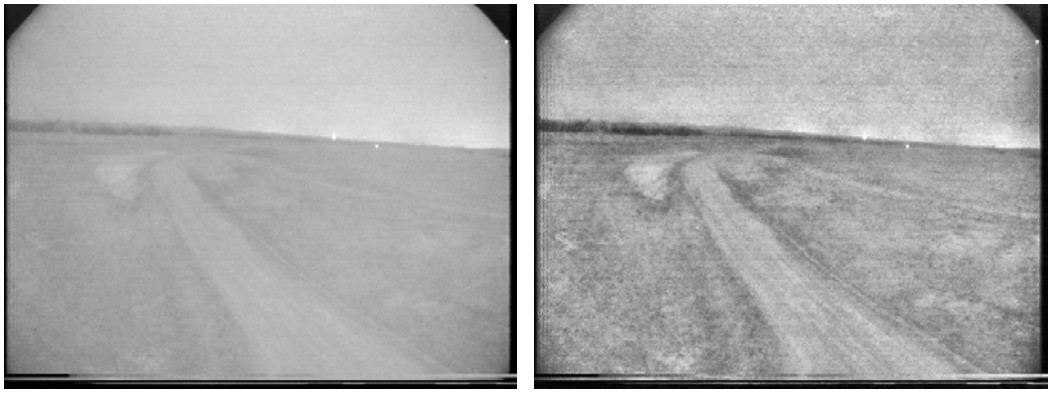

Image pair 19

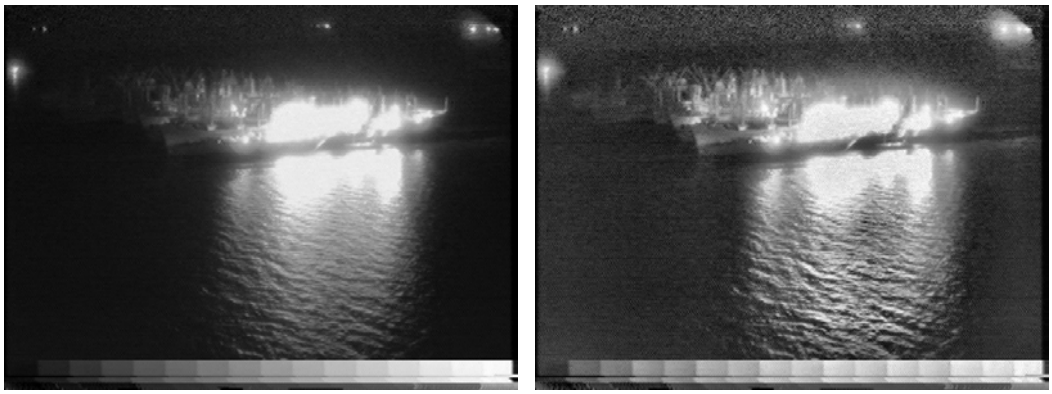

Image pair 20

THIS PAGE INTENTIONALLY LEFT BLANK

LIST OF REFERENCES

1. Anderson, R. and et al.. *Military Utility of Multispectral and Hyperspectral sensors*. IRIA State of the Art Reports. Nov 1994.

2. Barret, Harrison H. “Objective assessment of image quality: effects of quantum noise and object variability”. J. Opt. Soc. Am. A/Vol. 7, No. 7, 1266-1278. Jul 1990.

3. Bernas, Martin. “Image Quality Evaluation”. IEEE International Symposium on Video/Image Processing and Multimedia Communications. Jun 2002.

4. Federation of American Scientists. “Land Warrior”. [http://www.fas.org/man/dod-101/sys/land/land-warrior.htm]. Oct 2003.

5. Gonzalez, Rafael C. and Woods, Richard E.. *Digital Image Processing*. Addison-Wesley Publishing Company Inc.. 1993.

6. Holst Gerald C.. *Electro-Optical Imaging System Performance*. Third edition. SPIE, 2003.

7. Hypermedia Image Processing Reference, “HIPR Top page”. [http://www.dai.ed.ac.uk/HIPR2/hipr_top.htm]. Oct 2003.

8. International Telecommunication Union Radio-communication Recommendation, *Methodology for the subjective assessment of the quality of television pictures.* ITU-R BT.500-11, 2002.

9. Ji, Wei. “EO Systems and Technology Review”. [http://www.physics.nus.edu.sg/~phyjiwei/DTS5709.htm]. Sep 2002.

10. Korry Electronics Co.. “Introduction to NVIS”. [http://www.korry.com/nightshield/nvis_intro.htm]. Oct 2003.

11. LCEO Night Vision Equipment. “The principles of Night Vision”. [http://www.squonk.net/users/lceo/NVworks.htm]. Oct 2003.

12. Leszek, Wajnar. *Image Analysis Application in Material Engineering*. CRC Press. 1999.

13. MathWorks Inc.. “Toolboxes: Image Processing Toolbox”. [http://www.mathworks.com/access/helpdesk/help/toolbox/images/images.shtml]. Oct 2003.

14. McCourt, Mark E. “Spatial Frequency Analysis”. [http://www.psychology.psych.ndsu.nodak.edu/mccourt/website/htdocs/HomePage/Psy460/Spatial%20frequency%20analysis/Spatial%20frequency%20analysis.html]. Oct 2003.

15. National Instruments Co.. ”Fourier Transforms and Frequency Analysis”. [http://www.ni.com/support/labview/toolkits/analysis/analy3.htm]. Oct 2003.

16. Pedrotti, Frank L.S.J. and Pedrotti, Leno S.. *Introduction to Optics*. Second edition. Prentice Hall. 1993.

17. Sampson, Matthew T.. *An Assessment of the Impact of Fused Monochrome and Fused Color Night Vision Displays on Reaction Time and Accuracy in Target Detection.* Master’s Thesis, Naval Postgraduate School, Sep 1996.

18. Sasso, Claude R., Major. “Soviet Night Operations in World War II”. Combat Studies Institute, U.S. Army Command and General Staff College, Fort Leavenworth. Leavenworth Paper No. 6. Dec 1982.

19. Scrofani, James W. *An Adaptive Method for the Enhanced Fusion of Low-Light Visible and Uncooled Thermal Infared Imagery*. Master’s Thesis, Naval Postgraduate School, Jun 1997.

20. Seul, Michael and et al.. *Practical Algorithms for Image Analysis*. Cambridge University Press. 2000.

21. Therrien, C.W. and et al. “An Adaptive Technique for the Enhanced Fusion of Low-Light Visible with Uncooled Thermal Infared Imagery”. IEEE Intimetional Conference on Image Processing. pp 405 – 408, Oct 1997.

22. Xue, Z. and et. al.. “Fusion of Visual and IR Images for Concealed Weapon Detection”. v.2, pp. 1198-1205. 2002.

23. Zuiderveld, Karel. “Contrast Limited Adaptive Histogram Equalization”. Graphics Gems IV, pp. 474-485. Academic Press. 1994.

INITIAL DISTRIBUTION LIST

1. Defense Technical Information Center
   Ft. Belvoir, Virginia

2. Dudley Knox Library
   Naval Postgraduate School
   Monterey, California

3. Professor Monique P. Fargues
   ECE Department
   Naval Postgraduate School
   Monterey, California

4. Professor Alfred W. Cooper
   Physics Department
   Naval Postgraduate School
   Monterey, California

5. Professor Ronald Pieper
   Department of Electrical Engineering
   University of Texas
   Tyler, Texas

6. Professor Yeo Tat Soon
   Temasek Defence Systems Institute
   Singapore

7. Mr Teo Chek Koon
   Defence Science and Technology Agency
   Singapore